HUMBER BRIDGE FULL SCALE MEASURE CAMPAIGNS 1990-1991

JMW Brownjohn[1], M Bocciolone[2], A Curami[2], M Falco[2], A Zasso[2]

[1] Earthquake Engineering Research Centre, University of Bristol BS8 1TR UK, now at NTU, Singapore.

[2] Dipartimento di Meccanica, Politecnico di Milano, Pzza L da Vinci 20133 Milano

SUMMARY

The Humber Bridge was the subject of an extensive monitoring campaign during 1990 and 1991 during which a large body of experimental data describing the loading and response processes was obtained. Some 70 instruments were used to measure wind speed and direction together with displacement, acceleration, rotation and temperature of the structure. The aim of the exercise was to validate mathematical modelling of the response of long span bridges to wind and to provide a picture of the relationships between the loading and response parameters.

A full description of the instrumentation and monitoring arrangements is given together with some example results.

(Any proofs to be sent to:
J Brownjohn,
Nanyang Technological University,
School of Civil and Structural Engineering
Nanyang Avenue
SINGAPORE 2263
Fax 7910676)

HUMBER BRIDGE FULL SCALE MEASURE CAMPAIGNS 1990-1991

JMW Brownjohn[1], M Bocciolone[2], A Curami[2], M Falco[2], A Zasso[2]

[1] Earthquake Engineering Research Centre, University of Bristol BS8 1TR UK, now at NTU, Singapore.

[2] Dipartimento di Meccanica, Politecnico di Milano, Pzza L da Vinci 20133 Milano

1 INTRODUCTION

Reliable predictions of the dynamic and aeroelastic behaviour of flexible structures such as long span bridges are of great interest due to the severe wind induced vibrations that may arise in such structures not properly designed aerodynamically. Different approaches are used and the most satisfactory method of analysis is still the subject of research. It is vital that data from full-scale tests are available to validate and calibrate such analytical models.

Although there are several examples of tests on long span bridges[1-6] such tests have usually been performed with numbers of transducers and duration of monitoring both too limited to provide the adequate resolution, accuracy, reliability and statistical consistency of data. The closest parallels to the monitoring of a suspension bridge described here have used the Deer Isle Bridge[7] and the Ohnaruto Bridge[8] as their subjects.

The particular aim of these measurements was to provide sufficient data to validate modelling[9] of the wind-induced response of a 3km main span suspension bridge and were made for Stretto di Messina SpA by Politecnico di Milano, the University of Bristol and ISMES SpA, who enjoyed the complete cooperation of the Humber Bridge Board (HBB).

This paper concentrates on providing a comprehensive description of the measurement programme and instrumentation arrangements, followed by examples of the results obtained and correlations observed.

2 THE HUMBER BRIDGE: STRUCTURE AND ENVIRONMENT

The Humber Bridge (Fig. 1) was chosen for comparison of prototype response with analytical predictions for a number of reasons. It was the world's longest span operating at the time, the deck has a streamlined shape with well definable aerodynamic characteristics, the site location is rather windy in winter and spring and the bridge itself has already been subject of numerous analytical studies, model tests and full-scale tests.

2.1 Description of the site

The measuring campaigns were intended to investigate the aeroelastic behaviour of the bridge correlated to the wind structure, which is influenced by the site topographic and climatic features.

The Humber Bridge crosses the estuary of the River Humber 50 Km from the coast, and connects the towns of Barton and Hessle on the South and North sides of the river. The site topography is dominated by the long Humber Estuary, surrounded by flat land on the South and small hills on the North-West side, as shown in Fig. 2.

2.2 Typical macro and micro meteorology at the site

Being in the temperate latitudes of the Northern Hemisphere, the prevailing winds in the United Kingdom are the Westerlies which occur in sequences of cyclones as a result of geostrophic effects[10]. The cyclones tend to be deeper and to track further South in winter months leading to stronger winds and unsettled wet weather. The sequences of cyclones are interrupted by continental anticyclones with light winds, clear skies and low temperatures. In warm summer periods with generally light winds, cooling light (Easterly) sea breezes are not uncommon on the East coast.

In general the Western and Northern parts of the UK experience the strongest winds with the East being partly sheltered from Westerly winds. The spine of Pennine hills, and the Peak District to the South West shelter Humberside from Westerly winds which are thus generally reduced in magnitude compared with other parts of the UK. On the other hand, anticyclonic Easterly winds blowing in from the cold land masses of Eastern Europe are generally most severe on the low-lying East coast of the UK.

The most significant winds experienced during the monitoring exercise were of these two types. Figs. 3a,b show distributions of measured wind speeds against horizontal wind angle for both monitoring periods.

The severe storms of 26 January and 25 February 1990 when winds gusting to 48m/sec were recorded locally occurred just before the measurements began but, as shown in Fig. 3, the monitoring period was characterized by quite strong winds. The strongest Westerly winds reached almost 25m/sec, Easterly winds peaked at 18m/sec (both values are 512-second averages) and with a good variety of directions and turbulent intensities the data recorded are satisfactory for the understanding of the aeroelastic behaviour of the bridge.

The response of a structure depends not just on horizontal wind speed and direction but on turbulent intensity I of horizontal (incident) wind, vertical and lateral turbulence and spatial correlation. Westerly flows that arrive across the hills of central England are appear to be more turbulent than Easterly winds or sea breezes arriving across flat land and water. Measured I is increased for Northerly winds as shown in Fig. 3c,d for θ close to 270°, although this may be due in part to structural interference (tower wake).

2.3 Description of the bridge

After the Severn[11] and Bosporus[12] bridges the Humber Bridge[13], opened to traffic in 1981, is the third in a series of long span suspension bridges sharing important features such as streamlined low drag closed box-girder decks, flexible towers and inclined hangers. With low seismicity, Humber has concrete towers, while the side spans are unequal lengths, with the much longer Barton side span to the south.

The bridge accommodates dual two-lane carriageways with footpath/cycle tracks wide enough for maintenance and road vehicle access, giving a total width of 28.5m for a 4.5m depth. The bridge was built to design requirements of the time including capacity for a 180t vehicle and resistance to winds of 47m/sec on the deck and up to 66m/sec at the top of the towers.

The box deck is composed of 18.1m long prefabricated sections each having four equi-spaced bulkheads to improve torsional stiffness, and longitudinal stringers stiffening the roadway plate. Short, widened end box-sections interface to the A-frame rockers which prevent vertical and lateral movement at the towers and the DEMAG roller bearings which provide roadway continuity. Access inside the deck is possible from doorways at the end of each span and through inspection portholes in the upper surface. A manway allows passage between sections, and mains power, lighting and cable trunking is available inside. Great care is taken by HBB to keep the box-deck interior dry to prevent corrosion.

Access inside the towers is possible from foundation (pier) level, roadway level and deck level with elevators from pier level through upper portal level and ladder access to the tower tips and cable saddles.

One pair of inclined hangers per box section on each side connects the deck to the main cables via hinged sockets; the shorter cables in the central part of the main span attach to the deck singly via doubly hinged sockets.

2.4 Studies on the Humber Bridge

Humber has been the subject of quite a number of engineering studies:

1) Wind tunnel studies

Prior to construction, wind tunnel studies[14] were undertaken by National Physical Laboratory (now British Maritime Technology) to determine, for a number of possible designs, wind speeds for wind-excited oscillations of the suspended structure and time-average wind loads on the suspended structure and towers. As part of the present study a series of tests[15] were conducted using the wind tunnel of Salvi SpA in Milan to determine the aerodynamic coefficients of the as-built Humber deck section.

2) Analytical

Apart from any simulations at the design stage, analytical studies have been undertaken by the University of Bristol as part of a programme of work on the effect of significant separation of the support points (towers, anchorages) on the response of long span bridges to travelling earthquake waves[16]. Mathematical modelling undertaken by Politecnico di Milano has used the data obtained from the monitoring exercise for system identification of the aerodynamic coefficients of the deck[17] and for simulation of the traffic effects[18].

3) Field tests

A complete modal survey of the Humber Bridge was undertaken by the University of Bristol Earthquake Engineering Research Centre (EERC) over a two week period in 1985[19], during which a comprehensive description of the modal characteristics of the bridge was obtained in the form of natural frequencies, mode shapes and damping ratios for over a hundred modes in the main and side spans and two towers. Some information on the relationship of wind speed and response was also obtained. A parallel study[20] by the Building Research Establishment (BRE) used a large number of accelerometers monitoring over longer periods. EERC returned to the Bridge in 1986 to obtain wind data to be used as part of a Canadian investigation[21] and BRE returned to the Bridge in 1988[22] to further investigate the response of the bridge to wind.

4) Present study

The present series of studies begun in 1989 with a pilot study[23] using an optical displacement measurement system to test out the system and to determine the level of wind-induced displacements of such a long span bridge.

The subject of this paper is the experimental aspect of the two monitoring exercises of 1990 and 1991. The EERC parts of these exercises have been reported[24-26] and some data, information and results have also been published, with a brief overview[27] of the 1990 exercise, a description of the wind climate and its mathematical representation[28] and system identification of the aerodynamic coefficients[17]. The two optical displacement measurement systems employed in the 1990 monitoring have also been described in detail[29,30]

As well as the global behaviour of the bridge, wind-induced oscillations of the hangers have aroused some interest and these are reported elsewhere[31,32].

Despite all these studies there are still gaps and uncertainties in the understanding of the mechanisms of response, particularly at high wind speeds, and there is certainly justification for further long-term monitoring activities[33].

3 OBJECTIVES

The purpose of the measurements described here was to collect an exhaustive set of data on the wind characteristics and the correlated bridge dynamics, together with other significant information such as traffic induced vibrations and loads, wind and rain induced vibrations of hangers and static and thermal loads on the structure. In order to have a clear understanding of the response and a good correlation with the wind information (speed, direction, turbulence, integral scale) it was necessary to provide a rather complex set up of instrumentation and monitoring equipment with many transducers. In order to obtain data for strong wind conditions and have a statistically reliable data set it was necessary to monitor the bridge for several months. A continuous supervision was also needed during much of the monitoring due to the complexity of the system and the heavy weather conditions in which the optical and wind transducers had to operate.

4 MONITORING PROGRAMME

In phase one of the monitoring from early March to late May 1990, data from between 60 and 70 channels of instruments were recorded. The data recorded included displacement data obtained from the two different optical systems[29,30].

In phase two, from February to June 1991, a reduced configuration of 16-20 channels was targeted on key response parameters identified from analysis of the phase 1 data and a study of hanger vibrations was made[31].

Both phases of monitoring were aimed to start as early as possible in the year.

5 INSTRUMENTATION: LAYOUT

Fig. 4a shows the disposition of monitoring equipment and facilities along the span of the bridge and Fig. 4b uses a representative section to illustrate typical instrument locations.

5.1 Objectives

With the aim of describing the spatial and temporal character of the loading and response in the appropriate detail it was necessary to arrange for appropriate location of transducers and to provide for reliable and capacious data acquisition systems operating at optimal sampling rates. Sufficient measurement positions were used to characterise the loading and response over the entire main span and the data sampling rate was set to capture the significant frequency range of load and response.

5.2 Control room

The interior of the deck provides a clean and sheltered environment for setting up electrical equipment and so the control station was situated in the first main box section of the main span adjacent to the Hessle tower ('C'in Fig. 4).

5.3 Strategy for type and location of instruments

Locations for the instruments were chosen broadly on the following basis:

For the wind measurements it was necessary to record wind conditions in minimally disturbed flow and to characterise the coherence of wind. To do this, combinations of cup anemometers and vanes mounted with axes either vertical or longitudinal were installed on lamp-posts 10m above the centre-line of the roadway with spacing along the deck ranging from 36m to 1300m. In addition instruments were installed at the top of a tower and on a leading edge of the deck.

The bulk of the response measurements were to be made by servo accelerometers arranged to measure vertical and horizontal acceleration and by inclinometers measuring rotation. These devices were arranged in the deck and towers to provide adequate spatial resolution of the lowest vertical, torsional and lateral deck vibration modes, without locating them at nodes of the principal vibration mode shapes.

Optical systems were installed to record vertical and lateral displacement at two points on the main span so that the quasi-static or sub-modal response of the deck could be determined.

Since the hangers of the bridge are known to vibrate with significant amplitudes under certain conditions of wind and precipitation[31,32], instrumentation was installed on selected hangers.

Transducers to measure relative displacement at deck bearings, temperature of main cables and wind pressure were also installed.

5.4 Cabling and power supply

With instruments located throughout the main span and the adjacent Hessle tower it was necessary to run 35km of instrument cable along the trunking from the control room to the locations in the deck and tower closest to the chosen measurement positions or 'sections'. The signal cables were terminated in junction boxes in the control room and the sections.

While the power supply in the bridge is known to be quite reliable, to guard against power disruption a 1200VA uninterruptible power supply (UPS) was installed, with power supplies for equipment in the control room, through the deck and in the towers routed through this. In order to prevent ground loops two-core shielded instrument cable was used throughout with earth connections for all signals tied to a single earth post in the control room at the UPS outlet, together with all power supply earths.

5.5 Sections, transducers locations and codes

The as-built arrangement for the instrumentation is shown in Fig. 4 and Table 1. A scheme of coding designating section number, instrument type, disposition within the section and orientation was devised, as shown in Table 1. Many of the anemometers and vanes were located on lamp-posts and the section positions were revised slightly to align them with lamp posts accessible from inside the deck.

6 INSTRUMENTATION: TRANSDUCERS

All of the instruments described in the previous section were used in phase 1, and a subset of these plus three extra instruments were used in phase 2. Except where mentioned all of the instrumentation was installed by Politecnico di Milano.

6.1 Wind speed and direction

Three types of sensor were used:

1) Danjay Designs TW8204 combined anemometer and vane direction sensor

As determined by step response measurements[34] the length constant for this model of 3-cup anemometer is approximately 1.4m giving a -3dB point of 1.1Hz in a 10m/sec mean wind, although the analog output is of 1-second mean values internally sampled at 1Hz (hence good frequency response with a sharp cutoff). This unit was installed by EERC on a lamp-post at a height of 6m above the roadway.

2) Brookes & Gatehouse Ltd (B&G) type 152 cup anemometers and type 211 wind vanes.

These were sited at several positions on the deck and tower placed to measure horizontal wind speed and direction in vertical (angle of attack) and horizontal (compass bearing) directions. Fig. 5a shows an anemometer and pair of vanes installed on a centre span lamp-post. The anemometer step response has also been determined giving a length constant of 2.25m giving a -3dB point of 0.7Hz at 10m/sec (with continuous output hence smooth attenuation characteristic).

3) Pitot tube and dynamometer winglet

This unusual instrument ('the bird', Fig. 5b) was designed and built by Politecnico di Milano and consists of a rectangular aerofoil coplanar with the longitudinal and lateral axes of the deck. The wing was free to weather-vane about a vertical axis driven by its tail to align the pitot tube with the wind flow. The pitot tube on the body connected to a Schaevitz P-3000 differential pressure transducer provides a dynamic pressure signal (for determining wind speed) and the aerofoil attached to the body via a load cell generates a signal proportional to the lift force on the aerofoil. The characteristics for the aerofoil (lift coefficient versus angle of attack) were obtained from wind tunnel testing so that given the two signals for wind speed and lift force the angle of attack of the wind relative to the deck could be determined. Also, the bird was used to evaluate the averaged effects of the vertical turbulence on a wing-like object in order to obtain indirectly an estimate of the averaged low frequency vertical turbulence over a 1m span wing.

6.2 Acceleration

Apart from devices attached to the hangers, sensors were deployed in the main structure to detect motion from DC (0Hz) through the range of wind induced response:

1) Vertical

These were Sundstrand model 305b accelerometers with Sundstrand model 515b servo amplifiers, placed as shown in Fig. 4 to measure vertical acceleration in the deck and longitudinal or lateral acceleration in the tower.

2) Horizontal/rotational

Sensorex model 41200 inclinometers were used at sections 4, 8 and 9 while Columbia model SI-701B inclinometers were used at sections 11 and 13. The original aim of using inclinometers was to give a signal representing rotation of the deck about the longitudinal axis, but this signal was swamped by the dynamic lateral acceleration[30] which this type of instrument has previously been used to measure[19]. Even so, the mean value of the inclinometer signal could still be interpreted as a static torsional displacement or twist.

6.3 Deck displacements

Two separate optical systems were used to measure the lateral and vertical translational displacements of the main span and potentiometers were used to measure longitudinal displacements:

1) Optometers[29]

These devices were originally developed by ISMES for measuring deflections of buildings and transmission cables. They use a CCD (charge coupled device) array to detect sharp contrasts in images of the moving targets. In this case the targets were two vertical sodium tubes (for horizontal displacements) and two large rectangular white boards with a single horizontal black strip (for vertical displacement). One target of each type was fixed to each of the two deck service gantries at the centre and quarter span positions.

The optometers themselves used 2m focal length reflecting telescopes to focus the images, and the displacement signals were available in real time in digital or analog form.

The optometers were finally installed some time after the start of the monitoring. The main difficulty in their use arose due to unexpectedly large vertical drift of the deck which sometimes led to the edges of the vertical lamps and the entire horizontal strip moving out of the lens field of view, consequently there are gaps in the information from the optometers measuring the (respective) vertical and horizontal displacements. Problems also arose due to poor image quality during sunrise, sunset and foggy weather.

2) Vision system[30]

A 'vision system' developed by EERC for tracking of multiple visual targets at video frame rate (25Hz) was used to add to and corroborate the optometer data. The video source employed at Humber was a 1.6m focal length lens with a CCD video camera attached and sighted on a 400mm roundel target located adjacent to the optometer target (Fig. 6a). The vision system uses transputer microprocessors to grab images from a video source and run algorithms in parallel to locate the position in the image where the best match to a stored template image is obtained. The same algorithms use data on past target trajectories to anticipate the subsequent motion and improve the system capability.

The video system was operated during occasional site visits by EERC staff as an exercise separate to (but concurrent and synchronised with) the other forms of acquisition.

3) Deck longitudinal displacements

Relative displacement between the main span and each of the towers was measured by means of Celesco model PT101 pull-wire potentiometers. The units were attached between a handrail on the lower portal level and the access door, approximately located on the deck centreline. Only one transducer was installed in phase 1.

6.4 Main cable temperature

Solid state temperature sensors (type LM35DZ) were attached either side of the East main cable at its lowest position, at centre span. The transducers provide a Voltage signal proportional to temperatures above 0°C.

6.5 Hanger monitoring

Transducers were attached to hanger cables to measure wind and traffic induced vibrations.

1) Bending transducers

Bentley Nevada series 7200 proximeters (non-contacting displacement transducers) were installed to measure the bending of the hangers relative to the hanger socket in the transverse and longitudinal plane.

2) Acceleration transducers

Vibro-Meter series 500 piezoelectric accelerometers were attached to the hangers close to the sockets, also to measure in lateral and longitudinal directions.

3) Servo accelerometers

Sundstrand accelerometers were used in a one-off series of measurements[31] on the hangers to determine their modal characteristics and to calibrate the permanently installed proximeters and piezo accelerometers.

6.6 Calibration

For steady winds the B&G cup anemometers were calibrated in the Pininfarina (Torino) wind tunnel and the Danjay unit was calibrated in the University of Bristol Aerospace Engineering Department open section tunnel. Weather vanes were also calibrated for static and (for B&G units) dynamic response[35].

The optical displacement measurement systems were calibrated using the geometrical configurations of lenses and target[29,30] and against each other. The EERC system was also checked against a known target sizes. The Celesco potentiometers were calibrated against a metre rule and the proximeters were calibrated using thickness gauges.

The servo accelerometers were calibrated against gravity and the piezo-accelerometers were calibrated against servo-accelerometers.

Signal conditioning and data acquisition equipment was calibrated with test signals. Only the temperature gauges were not calibrated.

7 INSTRUMENTATION: SIGNAL CONDITIONING, ACQUISITION AND STORAGE

7.1 Overview

All the signals (except those from the video camera) were available in termination panels in the control room and were available to different systems of analog and digital acquisition installed by Politecnico di Milano and EERC.

Fig. 7 is a simplified block diagram of the signal conditioning and data acquisition arrangements. The subsequent section give details of the hardware and interconnections used in phases 1 ands 2.

1) Phase 1

All the instrumentation described in the previous section was installed during this phase with all but a few specific signals (Danjay wind sensors and vision system) acquired by the Politecnico di Milano equipment in the form of digital and analog signals. Sustained acquisition for a maximum of several hours was possible without manual changing of analog or digital storage media.

A digital data acquisition system was installed by EERC to monitor only eight signals but with sustained acquisition for a maximum of 24 days.

2) Phase 2

Only 20 transducers were installed, 16 of which were monitored continuously by the EERC digital system for sustained periods of up to 20 days. Analog recordings of a few hours duration were also made, triggered by high winds or large vibrations.

7.2 Digital data acquisition systems

Digital data acquisition was used in both phases, with two systems operating in phase 1 and only one of these operating in phase 2.

1) Computers, analog to digital conversion (ADC) and storage

The Politecnico di Milano system comprised a HP3852/11 analog to digital converter (ADC) controlled by a HP300 computer and set to sample signals at 6Hz per channel.

The HP3852 was arranged to monitor up to 68 channels, but a maximum number of 62 channels was finally used.

In order to record wind and response parameters relating to as many variations of wind conditions as possible, the HP300 was programmed to record data acquired via the HP3852 on a selective basis according to wind speed and compass bearing averaged over a 10-minute period (Fig. 8). For example if after storing data for a 10 minute period on HP9153 hard disk and computing mean direction and wind speed, these values corresponded to a sector for which no data had been recorded, the 10-minute complete data set would be recorded on tape via the HP9144 tape drive. To use up spare tape for speed/angle sectors not experienced, extra data corresponding to sectors representing high wind speeds would be recorded temporarily, being overwritten if data appropriate to the sectors became available. As an alternative, during periods of strong wind the full capacity of a tape was used to store complete 3½-hour time histories.

The EERC system comprised a Toshiba T5200 computer fitted with a Data Translation DT2821 16 channel ADC and a SCSI interface for a Panasonic LF5010E write once read many (WORM) optical disk drive. Eight channels were monitored in phase 1, sixteen in phase 2. The data acquisition was set to acquire at a sample rate of 8Hz per channels continuously over periods of up to 24 days, according to the 0.45GByte capacity per side of the WORM disks.

2) Sampling rate and anti-alias filtering

The sampling rates set the maximum data bandwidth (half the sampling rate) and low pass filters were used where appropriate to prevent aliasing, necessarily reducing the data bandwidth somewhat below half the sampling rate. In fact sampling rates and filter settings were chosen to preserve data in the range 0-1Hz at least, which corresponds to the useful range of wind induced response of the deck and towers. Because the bandwidth of interest for hanger vibrations is 0-10Hz these signals could not be digitised and the unfiltered signals were recorded only on FM analog tape.

All signals digitised by the EERC computer were filtered using 4-pole Butterworth low pass active filter modules with a -3dB point of 1.06Hz for phase 1 and 2.34Hz for phase 2. Accelerometer signals which included the significant accelerations above 2Hz due to traffic were doubly filtered (8-pole) with intermediate x10 amplification. All filters were fitted with differential inputs to preserve the single point grounding requirement.

Of the signals digitised by the HP3852, the servo-accelerometer, inclinometer, optometer and winglet signals were low pass filtered, at a range of frequencies. Signals from the anemometers and wind vanes were not filtered, trusting in the low pass characteristics of the instruments and the low noise over a strong signal. Temperature and Celesco signals were not filtered due to their low noise and low frequency.

7.3 Analog recorders

Analog recorders were used in both phases. In phase one a TEAC XR5000 was used to record 26 signals, 10 of these on FM channels, 16 of these on a pair of eight-channel pulse code modulated (PCM) channels with reduced bandwidth. In normal use these channels were used to record a representative selection of the 68 signals monitored by the HP300 while on occasion hanger signals were substituted for deck response signals.

In phase 2 all 20 channels of wind and acceleration data were recorded on FM and PCM channels. The recorder was set to trigger recording when wind speed exceeded a preset level (15m/sec).

In addition to the TEAC, a Racal Store 4DS four channel FM recorder was used to record four channels of hanger acceleration signals, representing two orthogonal directions of motion on two hangers. The recorder was triggered when the RMS acceleration of the hangers exceeded a preset level.

The TEAC recorded data on VHS video tape at a rate of 1.2inch/second giving a duration of 7 hours and a 313Hz bandwidth on FM and 9Hz bandwidth with PCM. The Racal was run at 0.9375inch/second giving a duration of over 7 hours and a bandwidth of 600Hz.

The video signals from the vision system were recorded on 1-hour U-matic professional quality video tapes.

8 ORGANISATION OF ANALYSIS OF ACQUIRED DATA

The recorded data comprised time histories in digital or analog form (which could be digitised in the laboratory). These time histories were used directly for validation of the time-history computations[9], for system identification of modal and aerodynamic parameters[17] or for identification of correlations between load and response. Examples of individual time histories are given in a subsequent section.

In the first two applications a relatively small amount of the data was used; in the third application all of the data were used in a systematic analysis and search for correlations.

In order to derive these correlations the recorded time histories were converted to engineering units and compressed as summaries of statistical properties (σ,μ etc.) over 512 or 600 second segments for data processed by EERC and Politecnico di Milano respectively.

Due mainly to aeroelastic effects, modal parameters are affected by the wind speed and turbulence[36]. Digital Fourier transforms (FFTs) for segments with similar wind speed, angle and/or turbulent intensity were averaged so that reliable estimates of modal parameters corresponding to the different conditions could be derived and trends established.

The data collected by EERC alone represents 3.5GBytes of disk storage. Special software was written in the ASYST language to process and organise the data as described above.

9 DATA ANALYSIS: TYPICAL RESULTS

The data obtained during the monitoring continues to be analysed and in a limited space it is possible only to show some of the more interesting relationships between the loading and response parameters.

The conventions used for the loading and response parameters as shown in this paper are illustrated in Fig. 1. θ is the angle in the horizontal plane between the wind and a perpendicular to the deck and increases in the sense of a compass bearing from 0° for a wind just North of East (due North is -85.5°). V is the wind speed signal from a cup anemometer and α is the angle of attack of the wind as sensed by a wind vane which rotates about a fixed longitudinal axis.

9.1 Wind conditions

The wind conditions during phase 1 have been described in detail elsewhere[28]. Fig. 3 shows distribution of wind speeds during phases 1 and 2, which showed similar ranges of wind speed. There were similar declines in extreme values as summer approached. The strongest winds (maximum gusts 30m/sec, 512-second averages up to 24.5m/sec) were from the West.

The variation of normalised wind power spectrum according to the wind direction will affect relationships between response and mean wind. Although information about the shape of the wind power spectrum is lost, turbulent intensity values I as shown in Fig. 3c,d help to show the directional effect. For both phases the dominant winds in the South West quadrant have I ranging around 3-11%, but North winds appear to be more turbulent in phase 2 measurements (Fig. 3c). In phase 1 the Danjay anemometer was 290m from the South tower and providing information up to 1Hz while for phase 2 measurements (Fig. 3d) the B&G anemometer was 180m from the North tower and with gradual filtering up to the 4Hz Nyquist frequency. The proportion of extra energy from 1-4Hz is not great so the higher turbulence measured by the B&G may be explained by the local flow disturbance by the tower.

9.2 Correlations established from 1990 data

Displacement response from DC to sub-modal frequencies is the combination of effects of wind, temperature and traffic loading. Modal response is due to wind and traffic with wind effects decreasing and traffic effects increasing with frequency.

Fig. 9 shows time histories of deck displacement in a strong wind on a weekend, obtained using the vision system. Fig. 10 shows correlation of 64-second average values of lateral and vertical deck displacement at mid span with wind speed, also from the vision system. Using the parabolic form of this data and a validated analytical model of the bridge[19], estimates of drag and lift coefficient can be obtained[30]. A moment coefficient can be derived from static rotation data.

The wind speed values plotted as the abscissae in Fig. 10 are the component of the wind speed normal to the deck, given by $V\cos\theta$, taking negative values for $90° > \theta > 270°$ i.e. mostly Easterly winds.

Fig. 11 shows diurnal variations of deck vertical and longitudinal displacement and main cable temperature at mid span, showing that temperature is in many cases the dominant effect. As temperature rises and the main cables expand, the deck drops and the span ends move towards the towers. Fig. 12 shows the geometric effect as the correlation of mid-span vertical deck displacement with longitudinal displacement.

The static displacements due to a Westerly wind and due to temperature are summarised in Fig. 13, with approximate coefficients of the appropriate parabolic or linear relationships with wind speed or temperature.

Fig. 14 shows the vertical displacement with the bridge closed to allow a single 172 tonne vehicle to cross; the superposition of scaled versions of this characteristic during periods of heavy goods vehicle traffic complicates interpretation of vertical displacement data. The displacements shown were measured using an optometer.

Using traffic data provided by HBB operations, Fig. 15 shows how RMS of vertical displacement at midspan (Fig. 15b) relates to the number of vehicles crossing the bridge per hour (Fig. 15a). There are clear peaks in the morning and evening rush hour periods and minimal response between 10pm and 5am. Fig. 15c is an example of an averaged FFT of vertical deck *acceleration* response up to 50Hz showing that response is usually dominated by traffic effects. These effects occur at frequencies which depend on the vibration characteristics of the sprung and unsprung vehicle masses[18] and are filtered out before digitising wind induced response in the 0-1Hz range. Even so, vehicular traffic clearly has a strong influence on static displacement response and produces similar levels of dynamic modal response to the very low frequency gusting of the wind up to 10m/sec. The clearest demonstrations of wind induced response derive from periods of low traffic (at weekends and in the small hours of the night).

9.3 Further observations from 1991 data

Some understanding of the effect of variable wind conditions can be judged from data obtained during a weekend in March 1991. During a period from 17.30 on the Saturday afternoon to 06.00 on the next (Sunday) morning the wind speed increased from 8m/sec to 24m/sec and dropped back to 12m/sec while the direction changed from approximately West of South ($< 180°$) to South of West ($> 90°$). The deck response is almost entirely due to wind, there being typically minimal traffic during this period of a weekend. Figs. 16-19 show the wind and response data for this period, in each case the ordinates are 512 second average values.

Fig. 16 shows the variation of a) speed, b) direction, c) normal component, d) angle of attack and e) I during this period. I and vertical angle of attack both reduce as the wind veers from South to West, although since the horizontal axis of the vane measuring vertical angle has a fixed alignment along the longitudinal (N-S) axis of the bridge the values of α for θ close to 90° are dubious.

Fig. 17 shows the variation of longitudinal displacement of the deck away from the towers during this period. Referring to Figs. 11a, 12 and 16a-c, the displacement is the combination of several effects:

1) as the deck cools the cables contract, the deck hogs and the ends move together.
2) as the wind increases the negative lift increases, the deck sags and the ends move apart
3) a wind component from the South along the deck pushes it towards Hessle.

Before midnight (24.00 hours) the contraction of the cable as it cools, the increasing negative lift force on the deck as the wind increases and the reducing Southerly wind vector sum to a net zero effect at the Barton end of the span with a slight movement away from the Hessle tower. After midnight (24.00 hours) the effect of 3) is minimal and the effects of 1 and 2 (when the wind decreases and the deck continues to cool) are additive.

Static torsional response of the deck is quite easily obtained from inclinometers and is not significantly affected by temperature or traffic. The relationship between wind speed and static deck rotation is clear from Fig. 18a (time history) and Fig. 18b (correlation with $V\cos\theta$).

It is generally assumed that the response of a bluff body in an incident wind is dependent on the vector $V\cos\theta$ rather than V. Fig. 18 shows how this applies to static torsional response but this does not seem to be the case for amplitude of dynamic acceleration response of vertical mode V1 (0.125Hz), as shown in Fig. 19a. Fig. 19b shows mode V1 response against absolute wind speed V showing a clearer relationship. The difference between the relationships shown in Fig. 18 and 19 is probably because the dynamic response also depends on the turbulence (Fig. 16e), which decreases as the wind veers, offsetting the effect of increasing normal wind. The varying angle of attack (Fig. 16d) also changes and this may affect the response in different ways.

9.4 Aeroelastic effects

The aeroelastic effects have been fully described elsewhere[17]. Fig. 20 shows an example of how modal amplitude, frequency and damping are affected by wind speed; the frequency of mode T1 at about 0.31Hz has been reduced and half-power bandwidth (proportional to damping) increased for the higher wind speed. Mode V1 shows a very much more pronounced dependence of measured damping on wind speed together with an increase in frequency with wind speed.

10 PRACTICAL DIFFICULTIES

Despite the complexity of the monitoring campaigns and the numerous organisations involved, few serious problems were encountered.

Both optical systems were new to this application and had limitations. The EERC vision system was a prototype and was only able to operate during visits of EERC personnel. Some data (less than 20%) was lost due to poor visibility (summer haze). For the optometers the field of view was less than the excursion of the deck resulting in intermittent data losses and occasional re-adjustments to alignment. Both systems have benefited from experience in the field and are being refined with optimised targets and self-adjusting light thresholds (optometers) or more robust algorithms and hardware (vision system).

Because of logistical problems both monitoring exercise started relatively late in the winter cycle so that some useful data relating to extreme load and response was missed.

While the data obtained are sufficient for the original aim of calibrating a mathematical model the majority of the data derive from Westerly winds, leaving 'gaps' in the data for other conditions. Obtaining reliable relationships between loading and response parameters requires large amounts of data over the widest possible range of the parameters, yet with a number of factors such as wind speed, compass bearing, turbulent intensity, temperature, traffic load etc. influencing the response, finding periods where most of the parameters have similar or minimal effect greatly reduces the number of data points defining the relationship.

11 CONCLUSIONS

The measurement campaigns have provided a large body of data describing the response of the bridge. The data has made it possible to understand the nature of the quasi-static and modal behaviour of the bridge. Interpretation of the modal data according to wind conditions has shown that the modal parameters for lower modes are strongly influenced by wind. Many of the relationships that have been derived are to be expected. Some of the not so obvious or surprising relationships are:

1) Traffic load is broadband dynamic excitation process and even for the lowest modes of vibration induces a level of response similar to that caused by winds up to 10m/sec.

2) The modal parameters (amplitude, natural frequency and damping ratio) for the lowest lateral, vertical and torsional modes are strongly affected by wind speed.

3) There are many loading parameters varying at any time and in order to define a reliable correlation of a response parameter with a single loading parameter it is necessary that all other loading parameters are kept constant (or limited in range). Even with many months of original data the proportion having so many parameters all in limited ranges will become vanishingly small and so some assumptions and compromises have to be made if any data is to be left.

12 ACKNOWLEDGEMENTS

The Humber Bridge monitoring campaign has been part of a wider research program on long span suspension bridge dynamics and aeroelasticity going on at the Department of Mechanics of Politecnico di Milano, in cooperation with Society Stretto di Messina SpA., concerned with the Messina Crossing Project. The measuring campaign has been carried out jointly by Politecnico di Milano and the Earthquake Engineering Research Centre at the University of Bristol, with the assistance and cooperation of the Humber Bridge Board. Optoelectronic instrumentation monitoring the bridge displacements was supplied and operated by ISMES (Italy). The whole operation was financially supported by Society Stretto di Messina SpA., MURST and CNR (Italy), and SERC (UK). The support from the institutions mentioned above and the good cooperation and patience of all the participants on site, is gratefully acknowledged.

Fig. 2 is reproduced from ref. 19 courtesy of TTL London.

13 REFERENCES

1 A. M. Abdel-Ghaffar, R. H. Scanlan, 'Ambient vibration studies of Golden Gate Bridge: 1. Suspended structure'. *J. eng. mech. div. ASCE*, 1985, **111**, 463-482.

2 J. M. W. Brownjohn, A. A. Dumanoglu, R. T. Severn, A. Blakeborough, 'Ambient Vibration Survey of the Bosporus Suspension Bridge', *Earthquake eng. struct. dyn.*, 1989, **18**, 263-283.

3 J. M. W. Brownjohn, A. A. Dumanoglu, R. T. Severn 'Ambient Vibration Survey of the Fatih Sultan Mehmet (Second Bosporus) Bridge.', *Earthquake eng. struct. dyn.,* 1992, **21**, 907-924.

4 P. G. Buckland, R. Hooley, B. P. Morgenstern, J. H. Rainer, A. Van Selst, 'Suspension bridge vibrations: computed and measured.' *J. struct. div. ASCE*, 1979, **111**, 859-874.

5 V. R. Maclamore, G. C. Hart, I. R. Stubbs, 'Ambient vibration response of two suspension bridges.' *J. struct. div. ASCE*, 1971, **97**, 2567-2582.

6 I. Okauchi, A. Tanaka, K. Iwaya, N. Furuya, 'Vibration test of Ohnaruto test to confirm wind-proofness' *IABSE Symposium: Safety and Quality Assurance of Civil Engineering Structures,* Tokyo, 4-6 Sep. 1986, 52-55.

7 T. Kumarasena, R. H. Scanlan, G. R. Morris, 'Deer Isle Bridge: field and computed vibrations.' *J. struct. div. ASCE*, 1989, **115**, 2313-2328.

8 Observation of Ohnaruto Bridge Behaviour. Honshu Shikoku Bridge Authority, Japan, May 1987.

9 A. Curami, M. Falco 'The dynamic behaviour of a large span suspension bridge. Part 2 : Dynamic response to turbulent wind, *Costruzioni Metalliche*, (Milan, Italy), 1982, **34**, No. 2, 59-78.

10 R. C. Sutcliffe, *Meteorology for aviators.* M.O. 432 (A.P. 1699). HMSO 1946.

11 G. Roberts 'Severn Bridge: design and contract arrangements' *Proc. Instn Civ. Engrs,* 1968, **41**, 1-48.

12 W. C. Brown, M. F. Parsons, 'Bosporus Bridge Part 1: History of design', *Proc. Instn Civ. Engrs, Pt. 1*, 1975. **58**, 505-567.

13 Engineering the Humber Bridge. The Hillingdon Press, Uxbridge Middx.

14 D. E. Walshe, C. F. Cowdrey, *A further aerodynamic investigation for the proposed Humber Suspension Bridge.* National Physical Laboratory Maritime Science Report R102, June 1972.

15 M. Falco, A. Curami, A. Zasso, 'Nonlinear effects in sectional model aeroelastic parameters identification.' *J. Wind Eng. Ind. Aero,* 1992, **42**, 1321-1332.

16 A. A. Dumanoglu, R. T. Severn, 'Asynchronous seismic analysis of modern suspension bridges to travelling vertical ground motion.' *Proc. Instn Civ. Engrs, Pt. 2*, 1987, **83**, 701-730.

17 F. Cheli , A. Collina, G. Diana, A. Zasso, Brownjohn J M W, 'Suspension bridge parameter identification in full-scale test.' *J. Wind Eng. Ind. Aero,* 1992, **41**, 165-176.

18 F. Cheli , C. Porcu, 'Traffico stradale su ponti di grande luce: interazione dinamica. Modello analitico e risultati sperimentali.' *XI Congresso Nazionale AIMETA,* Trento, Italy, 1992.

19 J. M. W. Brownjohn, A. A. Dumanoglu, R. T. Severn, C. A. Taylor, 'Ambient vibration measurements of the Humber Suspension Bridge and comparison with calculated characteristics.' *Proc. Instn Civ. Engrs, Pt. 2,* 1987, **83**, 561-600.

20 J. D. Littler, B. R. Ellis, 'Ambient vibration measurements on the Humber Bridge.' *Conference on Flow Induced Vibrations*, Keswick, 1987.

21 G. Larose, J. P. C. King, A. G. Davenport, 'Wind effects on long span bridges: consistency of wind tunnel results.' *J. Wind Eng. Ind. Aero,* 1992, **42**, 1191-1202.

22 J. D. Littler, 'Ambient vibration tests on long span suspension bridges' *J. Wind Eng. Ind. Aero,* 1992, **42**, 1359-1370.

23 G. A. Stephen, 'Visual determination of ambient wind induced deflections of the Humber Bridge at mid span.' Report UBCE-EE-90-07, University of Bristol Department of Civil Engineering, Dec. 1989.

24 EERC, Humber Bridge monitoring: Optical deflection measurements March-May 1990, Report No. UBCE-EE-90-09, University of Bristol Department of Civil Engineering, July 1990.

25 J. M. W. Brownjohn, 'Humber Bridge Monitoring: Digital Measurements March-May 1990 And Preliminary Analysis.' Report UBCE-EE-90-10, University of Bristol, July 1990

26 'Humber Bridge monitoring: Digital measurements February-June 1991.' Report UBCE-EE-91-13, University of Bristol, Sep. 1991

27 G. Diana, M. Falco, R. T. Severn, M. L. Stockwell, 'Wind effects on a long span suspension bridge.' *9th Structures Congress,* Indianapolis, Indiana, 29 Apr.-1 May 1991.

28 A. Curami, F. Cheli, M. Bocciolone, A. Zasso, 'Wind Measurements on the Humber Bridge and Numerical Simulations.' *J. Wind Eng. Ind. Aero,* 1992, **42**, 1393-1404.

29 A. Zasso, M. Vergani, M. Bocciolone, R. Evans, 'Use of a newly designed optometric instrument for long-term, long distance monitoring of structures, with an example of its application on the Humber Bridge.' *2nd International Conference on Bridge Management*, 18-21 Apr. 1993, University of Surrey, UK.

30 G. A. Stephen, J. M. W. Brownjohn, C. A. Taylor, 'Visual monitoring of the Humber Bridge'. *Engineering Structures*, 1993, **15**, No. 3, 197-208.

31 A. Zasso, M. Bocciolone, J. M. W. Brownjohn, 'Rain-wind induced instability of the inclined hangers of a suspension bridge.' *Wind Engineering Society Inaugural Conference, Cambridge*, Sep. 1992.

32 M. L. Stockwell, R. A. Evans, N. J. Cherry, 'Hanger cable oscillations on the Humber Bridge.' *5th International Conference on Flow Induced Vibrations* (I.Mech. E), 20-22 May 1991, Brighton.

33 S. K. Sarma, J. Mitchinson, 'Wind induced response of suspension bridges' BEng Thesis, University of Bristol Department of Civil Engineering, May 1992.

34 C. J, Wood, 'Calibration of a TW8204 combined wind speed and direction sensor for Danjay Designs.' Oxford University Engineering Laboratory Report OUEL 1417/82, 1982.

35 Cigada A, Curami A, 'Analisi della riposta di uno strumento per la misura della turbolenza del vento.', Politecnico di Milano, Sezione Meccanica dei Sistemi, 1992.

36 D. R. Huston, 'The Effects of Upstream Gusting on the Aeroelastic Behaviour of Long Suspended-Span Bridges', Doctoral Dissertation, Princeton University, May 1986.

Table 1 Instruments and locations for data acquisition

Section No. →	0/00	1	3	4	5	6	7	8	9	10	11	12	E	13	14	15
Metres from Hessle tower →	0/1410	54	199	235	271	415	488	524	705	886	922	1030	1120	1175	1355	tower top
B&G cup anemometer ∪		WSH-1C	WSH-3C	WSH-4C	WSH-5C	WSH-6C WSH-6W		WSH-8C	WSH-9C	WSH-10C		WSH-12C		WSH-13C	WSH-14C	WSH-15C
B&G vane (vertical) ↑, (horizontal) →		WAV-1C	WAV-3C	WAV-4C WAH-4C	WAV-5C	WAV-6C WAV-6W		WAV-8C	WAV-9C WAH-9C	WAV-10C		WAV-12C		WAV-13C WAH-13C		WAH-15W
Danjay cup and vane ∪,→													WSH-EC WAH-EC			
Pitot tube ◊						WPH-6W										
Dynamometer winglet ♦						WLV-6W										
Servo-accelerometer ⇑,⇒				DGV-4W DGV-4E			DGV-7W DGV-7E		DGV-9W DGV-9E		DGV-11W DGV-11E			DGV-13W DGV-13E		TGL-15W TGN-15W
Inclinometer ∠				DGH-4C			DGH-7C		DGH-9C		DGH-11C			DGH-13C		
Piezo-accelerometer ⇔		HGL-1E HGN-1E	HGL-3E HGN-3E													
Proximeter ∩		HBL-1E HBL-1W* HBN-1E HBN-1W*	HBL-3E HBN-3E													
Optometer ∧,<						DDV-6C			DDV-9C DDH-9C							
Vision system ∇									DDV-9W DDH-9W							
Potentiometer ∩	DDN-0C DDN-00C*															
Temperature transducer°									CTS-9W CTS-9E							

KEY:

structure
D: deck
H: hanger
T: tower
W: wind
C: cable

parameter
A: angle
H: bending
D: displacement
G: acceleration
L: lift
P: pressure
S: speed
T: temperature
B: bending

orientation
H: horizontal
L: lateral
N: longitudinal
T: torsional
V: vertical
S: surface

section. No.

Position in section
C: central
E: East
W: West

e.g. WAV-6C is wind angle vertical in centre-line position (lamp post) in section 6.
WAV-3C signifies used in phases1,2, DDN-00C* used in phase 2 only

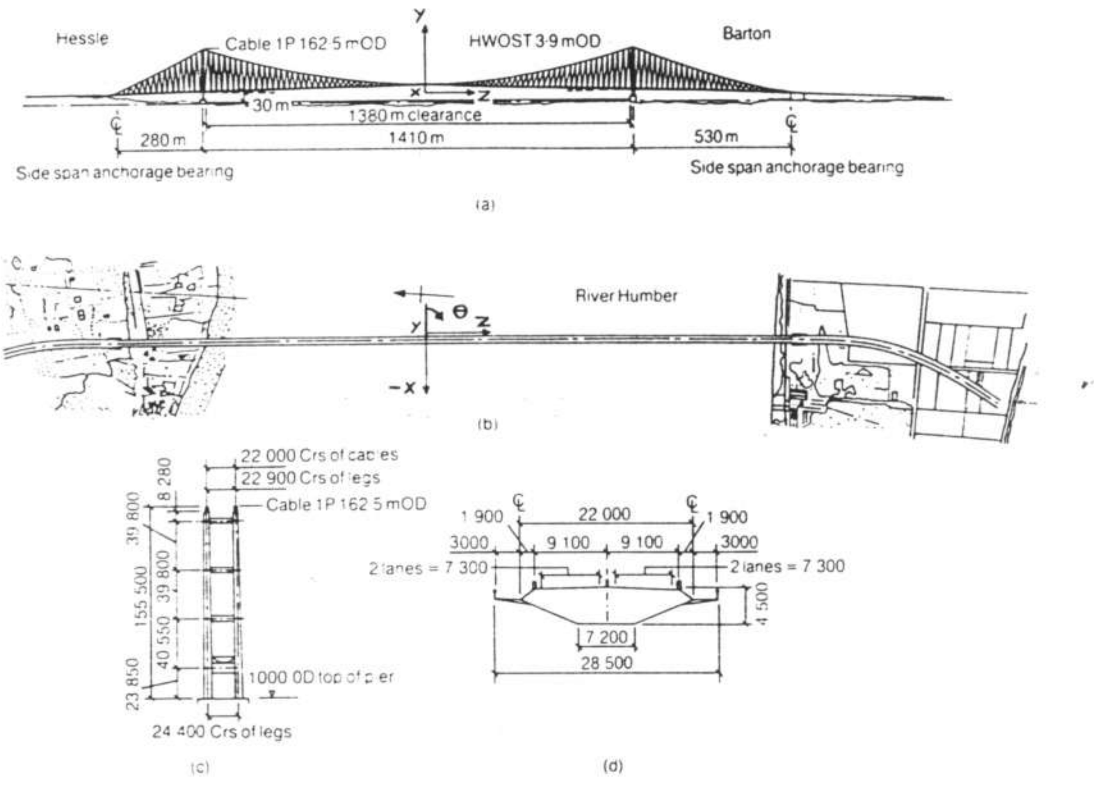

Fig. 1 Humber Bridge:

a) elevation b) plan c) towers d) deck section

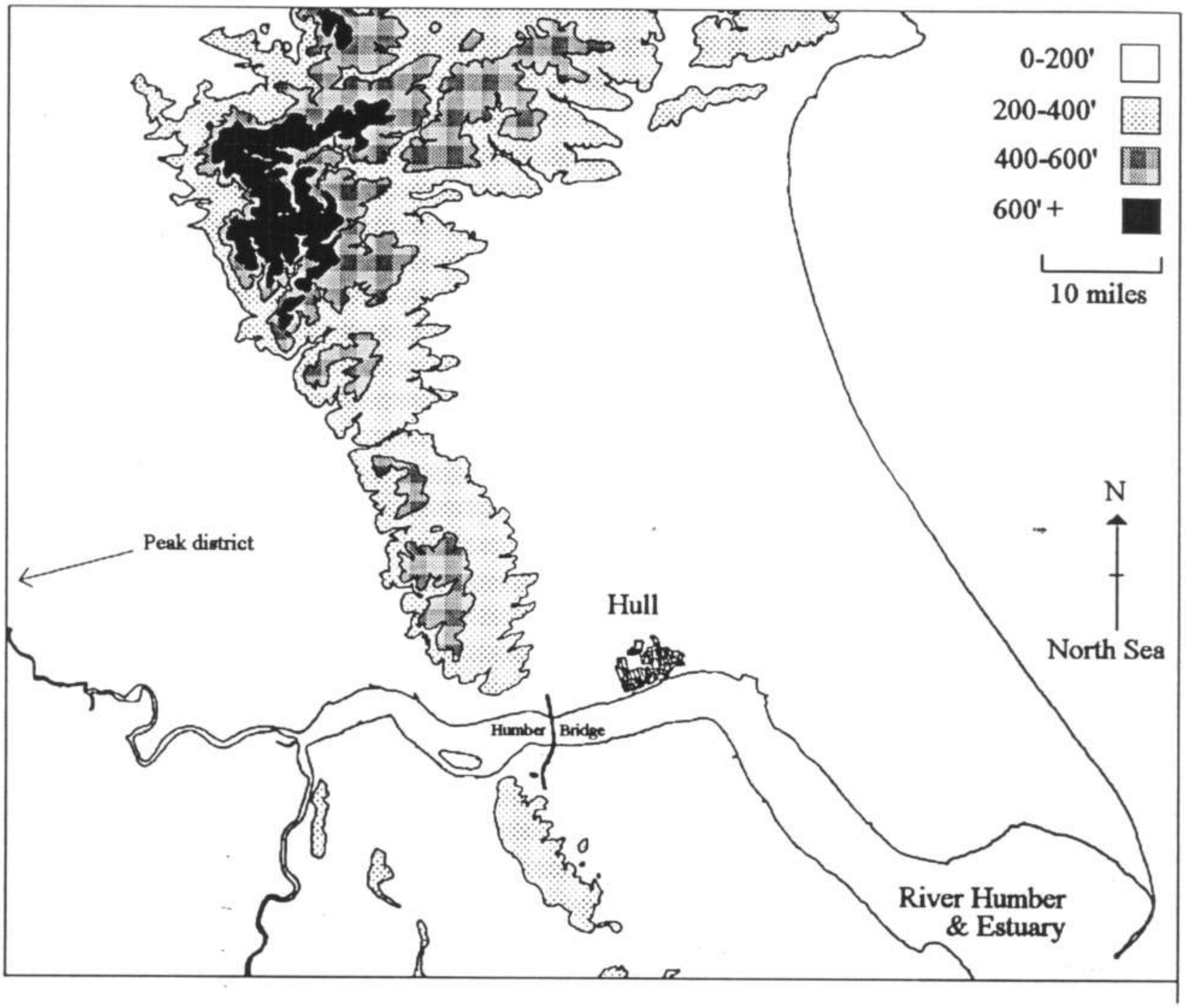

Fig. 2 Humberside Topography

Based on Bartholomews 1/4" scale map with permission of Her Majesty's Stationery Office, Crown Copyright Reserved

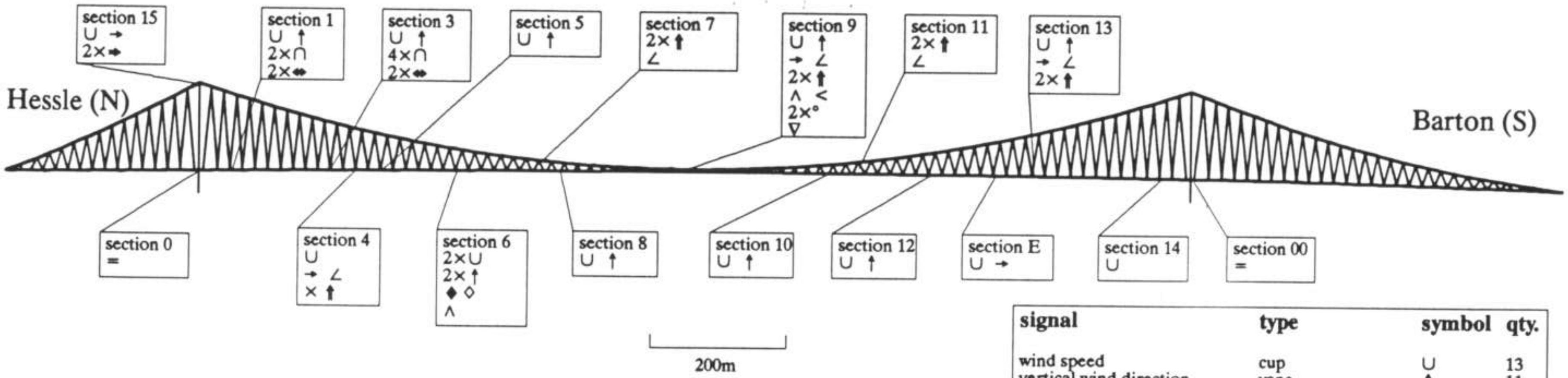

signal	type	symbol	qty.
wind speed	cup	∪	13
vertical wind direction	vane	↑	11
horizontal wind direction	vane	→	4
vertical lift force	winglet	◆	1
wind pressure	pitot tube	◇	1
vertical acceleration	servo acc.	⬆	10
horizontal acceleration/	servo acc.	➡	2
section angle	inclinometer	∠	5
hanger acceleration	piezo acc.	⬌	4
hanger bending	proximeter	∩	6
vertical displacement	optometer	∧	2
horizontal displacement	optometer	<	1
section displacement	vision	∇	1
longitudinal displacement	potentiometer	=	2
temperature	solid state	°	2

Fig. 4a Humber Bridge instrumentation types and locations

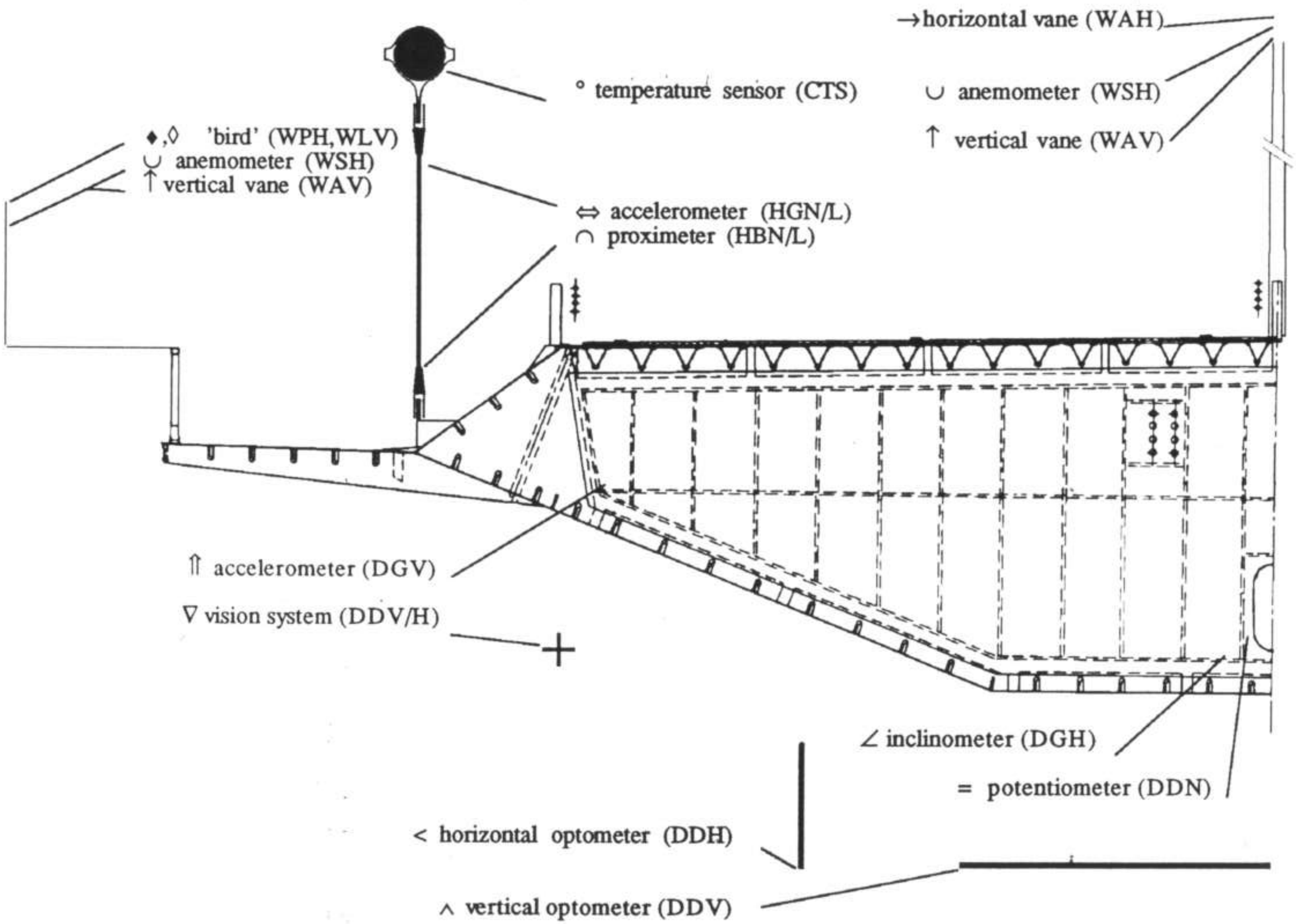

Fig. 4b Composite view of instrument locations across a section

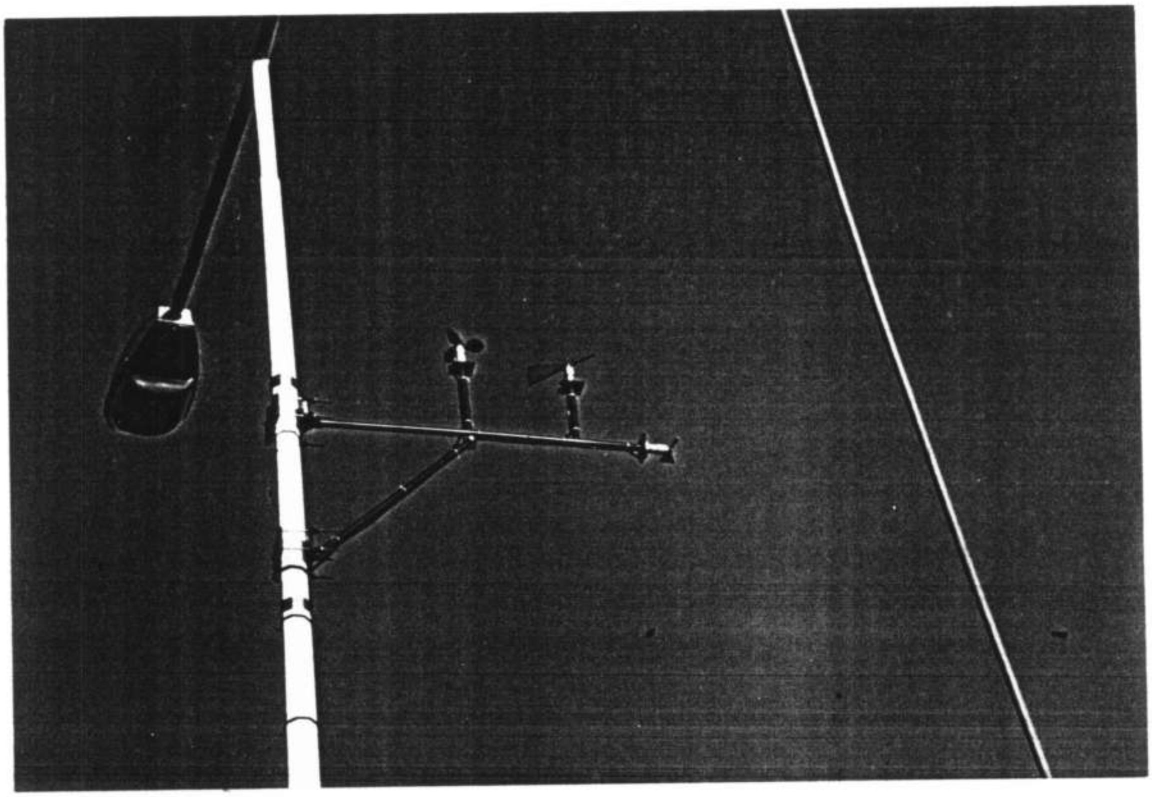

Fig. 5a Installation of cup anemometer and vanes on lamp post

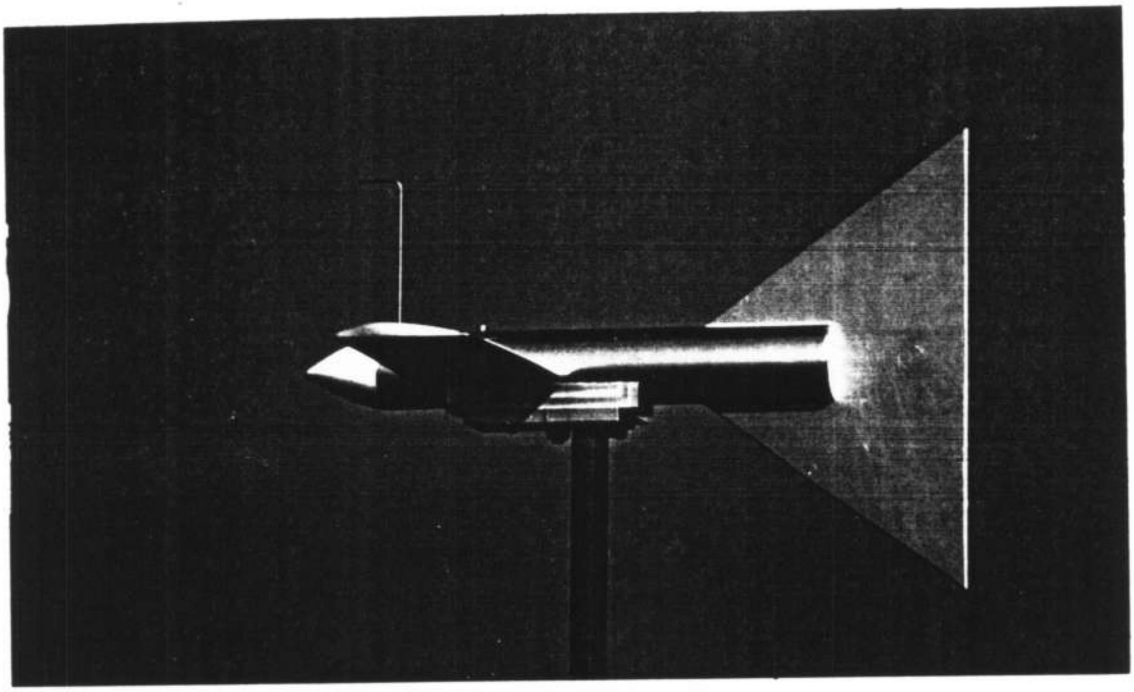

Fig. 5b Pitot tube and winglet ('the bird')

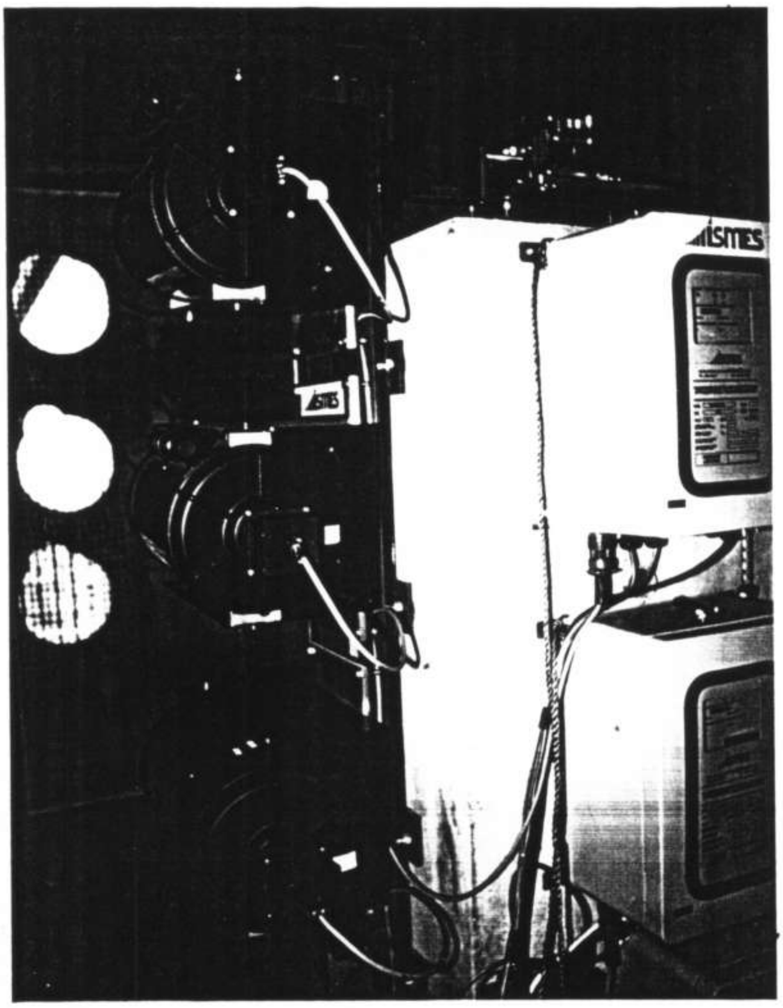

Fig. 6a Optometer lenses at base of Hessle tower (vision system lens removed)

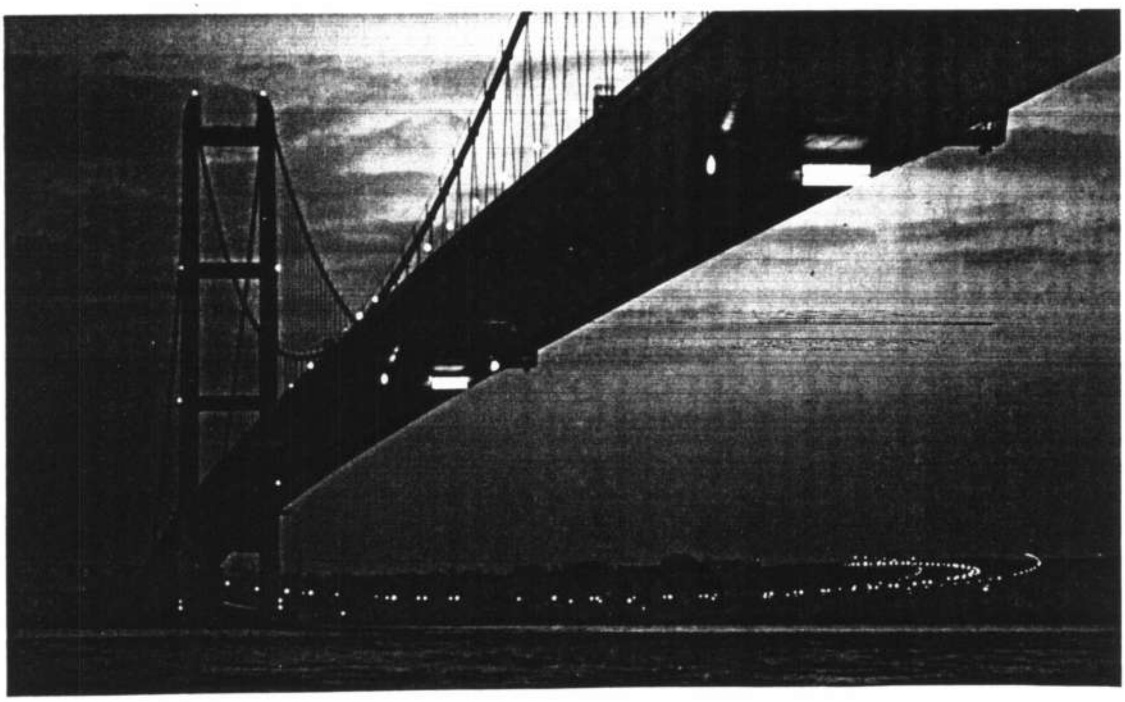

Fig. 6b Service gantries carrying horizontal, vertical optometer targets at quarter, mid span and vision system target at midspan

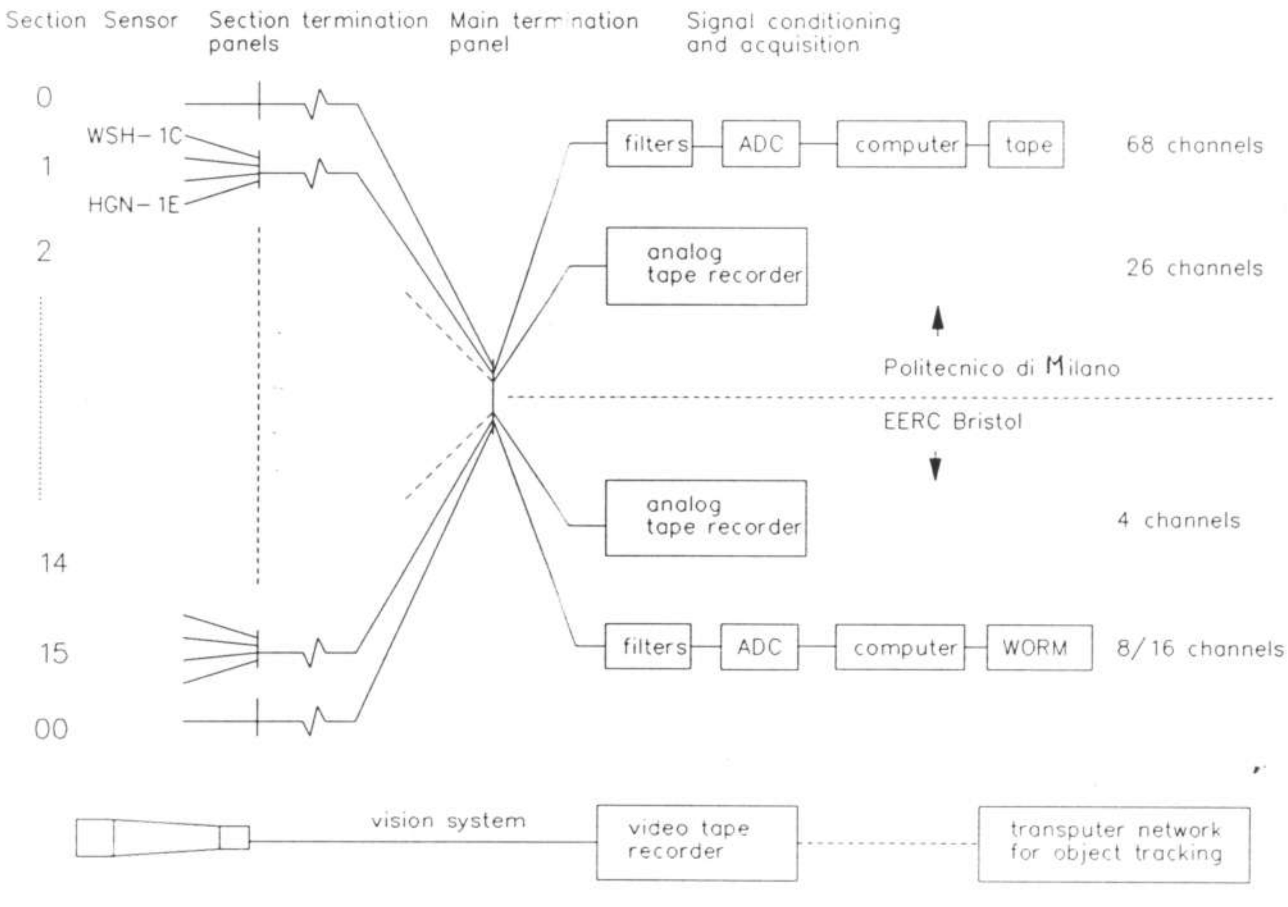

Fig. 7 Overview of data acquisition system

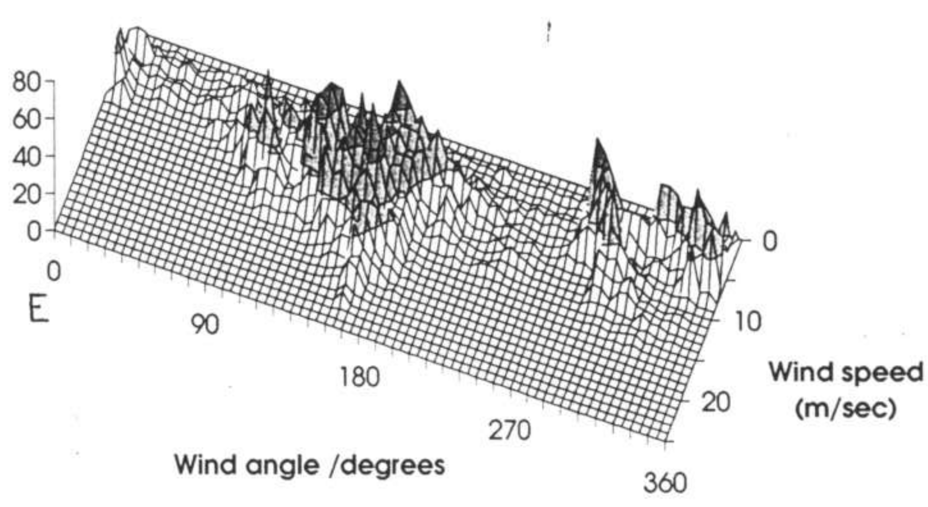

a) Wind speeds, phase 1

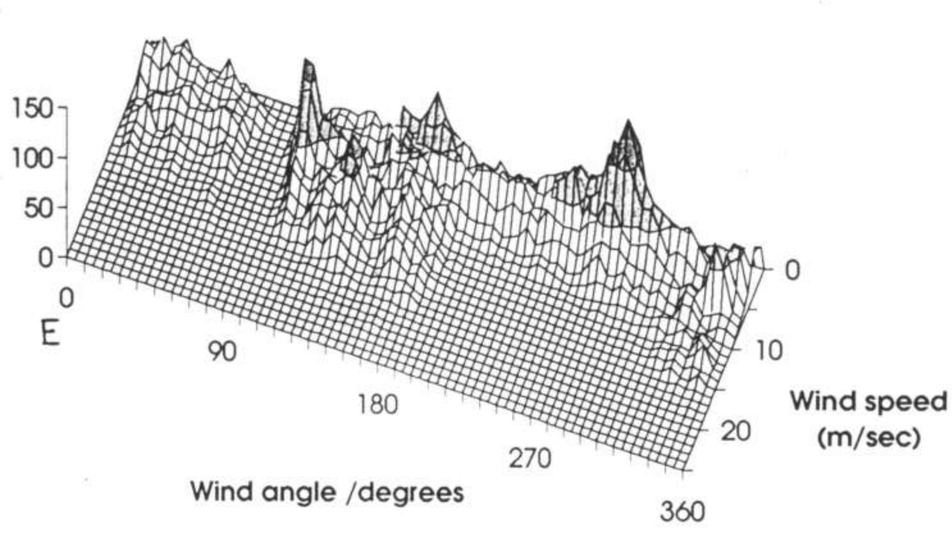

b) Wind speeds, phase 2

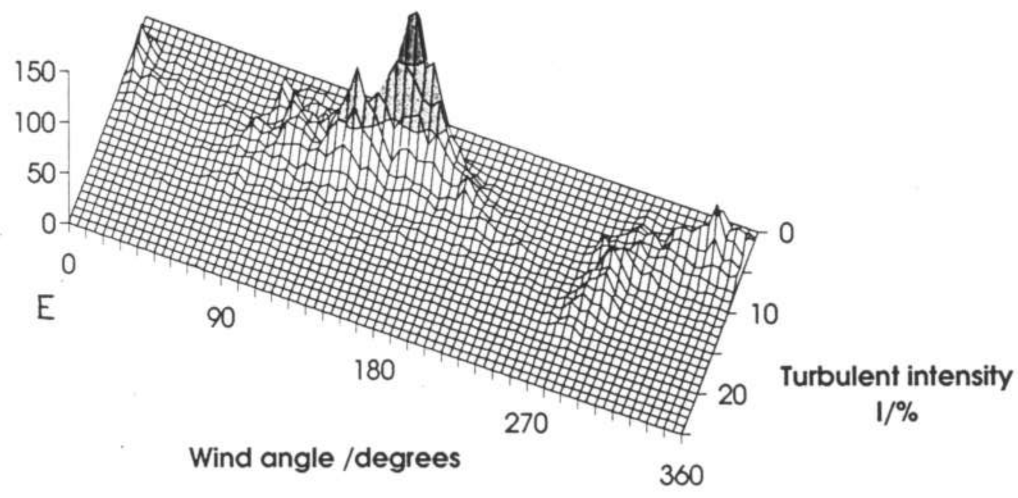

c) Turbulent intensity, phase 1

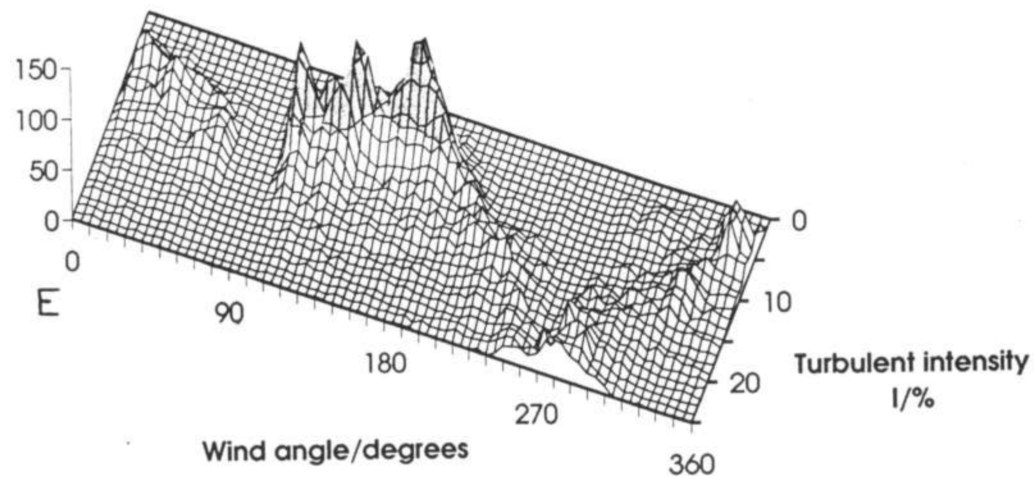

d) Turbulent intensity, phase 2

Fig. 3 Distribution of wind by speed V and turbulent intensity I. Wind angle θ is 0° for compass bearing 85.5° (≈ East).

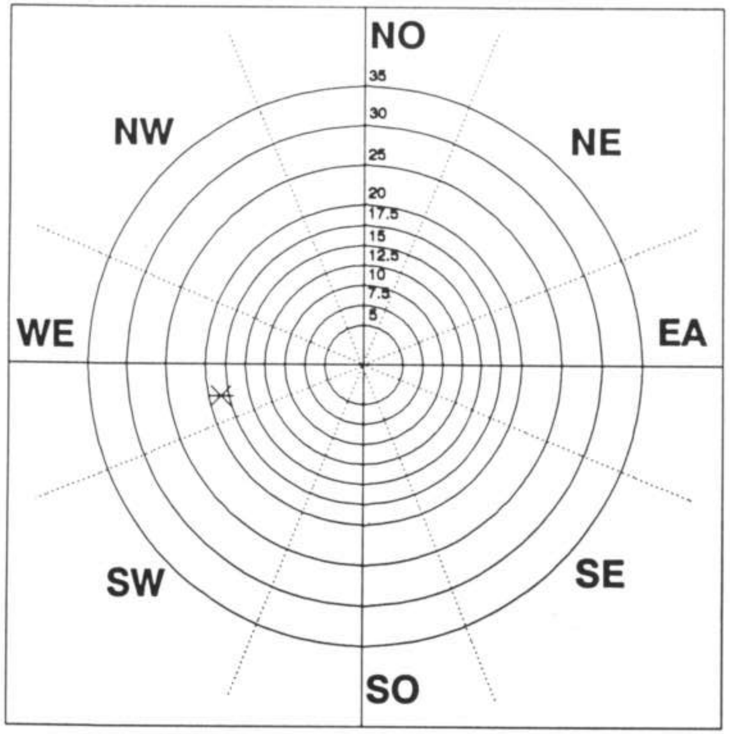

m/sec	EA	NE	NO	NW	WE	SW	SO	SE
5.0 → 7.5	7	6	7	7	7	7	7	••
7.5 → 10.0	10	10	10	10	10	10	10	••
10.0 → 12.5	10	11	11	12	12	12	12	••
12.5 → 15.0	••	••	••	••	13	15	14	••
15.0 → 17.5	••	••	••	••	17	17	••	••
17.5 → 20.0	••	••	••	••	18	••	••	••
20.0 → 25.0	••	••	••	••	••	••	••	••
25.0 → 30.0	••	••	••	••	••	••	••	••
30.0 → 35.0	••	••	••	••	••	••	••	••
> 35.0	••	••	••	••	••	••	••	••

bearing 245°   mean speed 18.1m/sec

Data 'sectors' stored on disk, plus new sector.

Fig. 8 Selection of acquired data records for storage by HP300 based on speed and direction criteria.

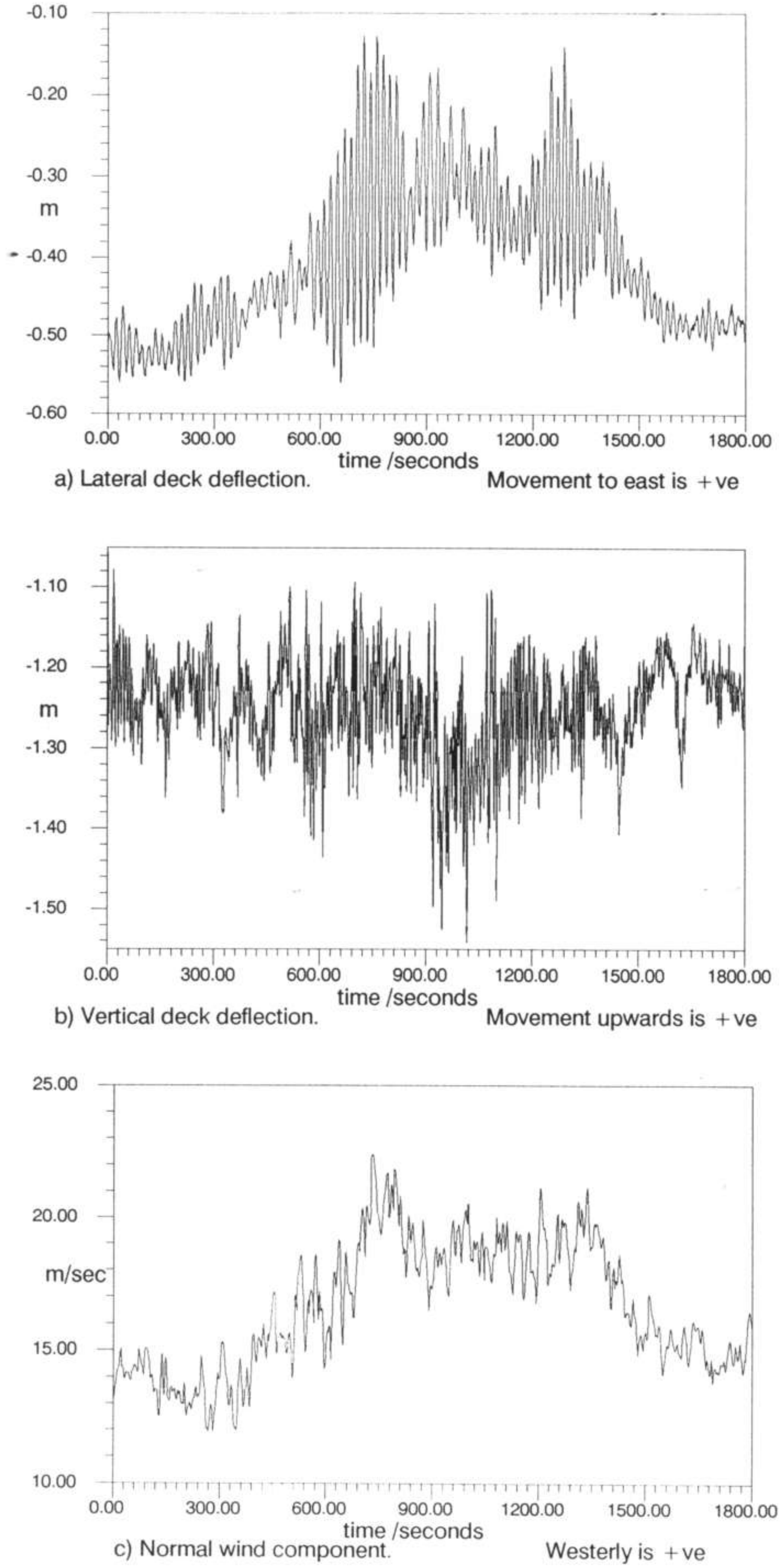

Fig. 9 Time histories at midspan, Saturday 24/3/1990

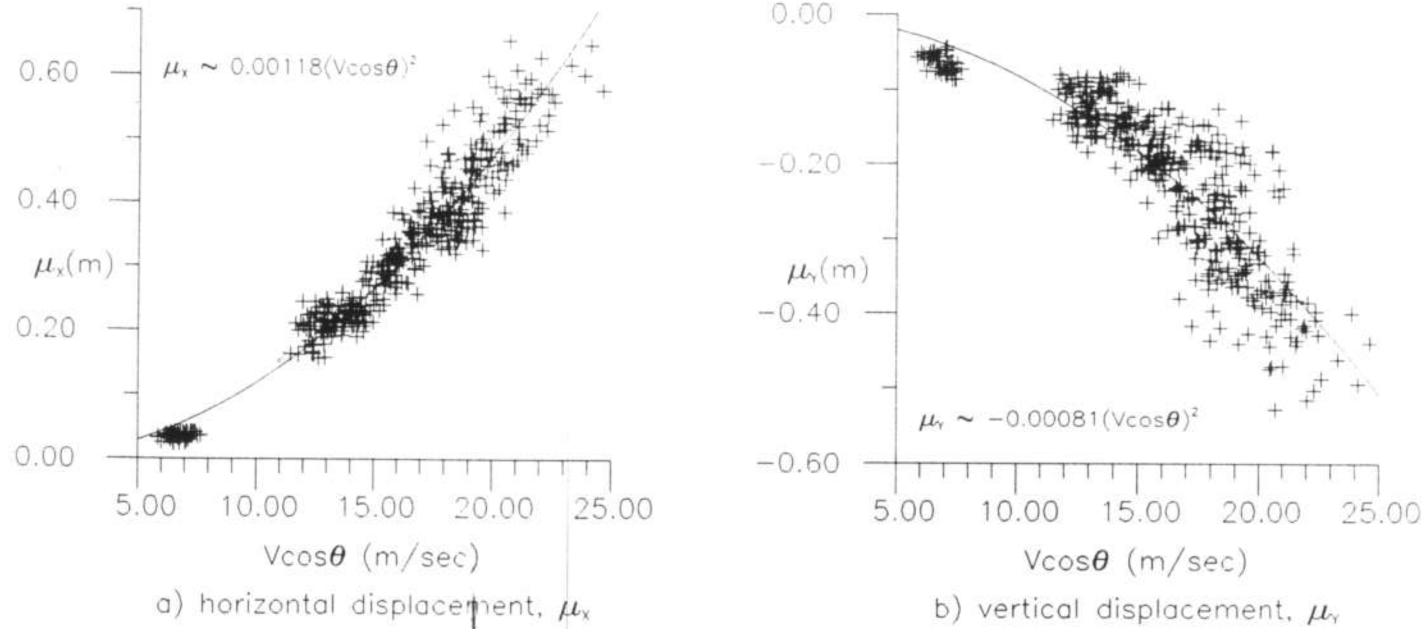

Fig. 10 64-second average values of normal wind vector vs lateral and vertical deck displacements at mid span. The μ_x, μ_y origins are arbitrary and are taken as 0 at V = 0 for illustration.

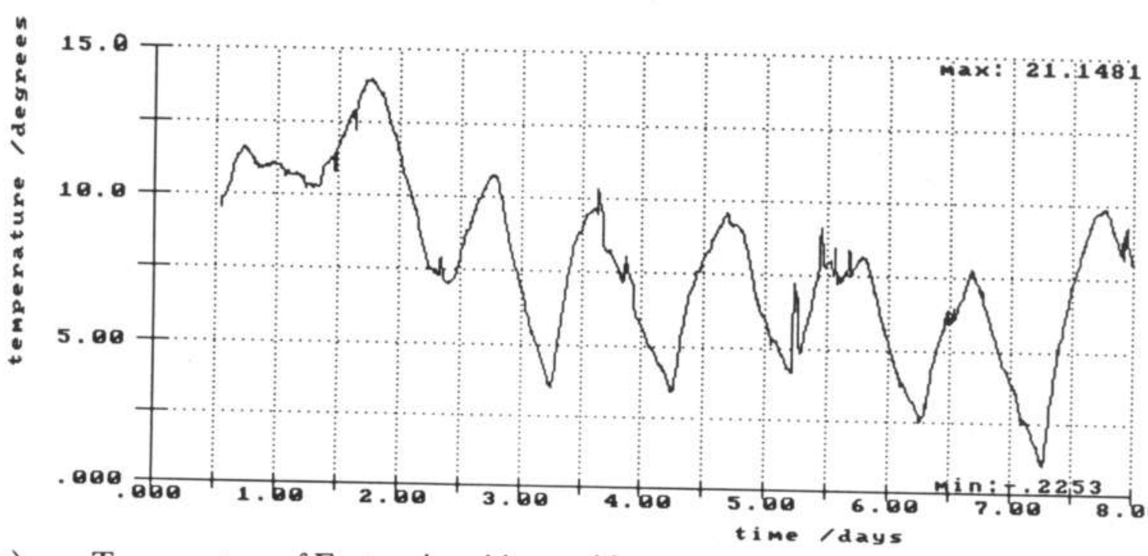

a) Temperature of East main cable at mid-span

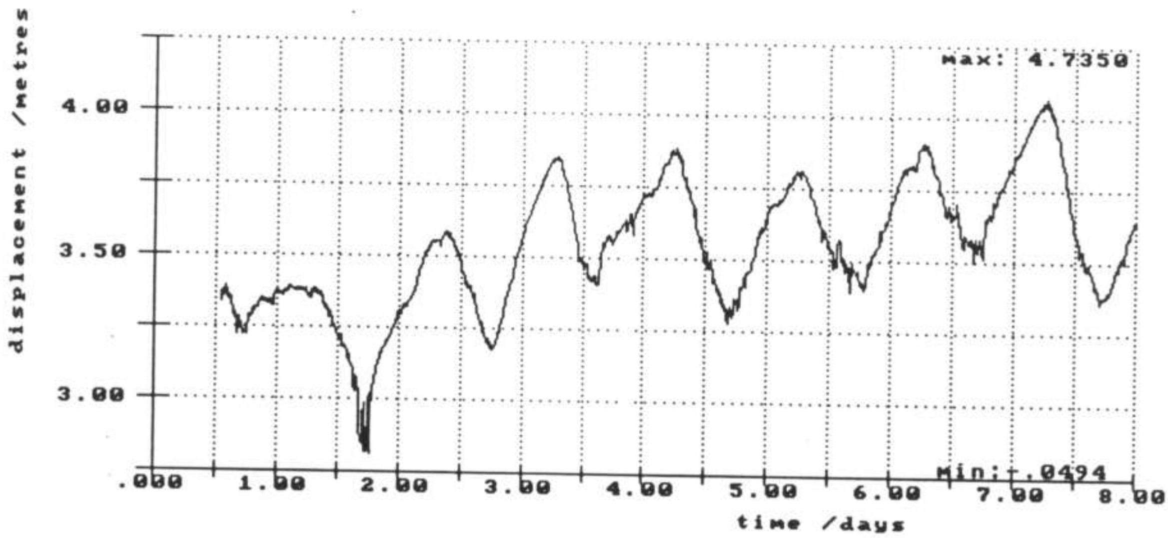

b) Vertical displacement at midspan

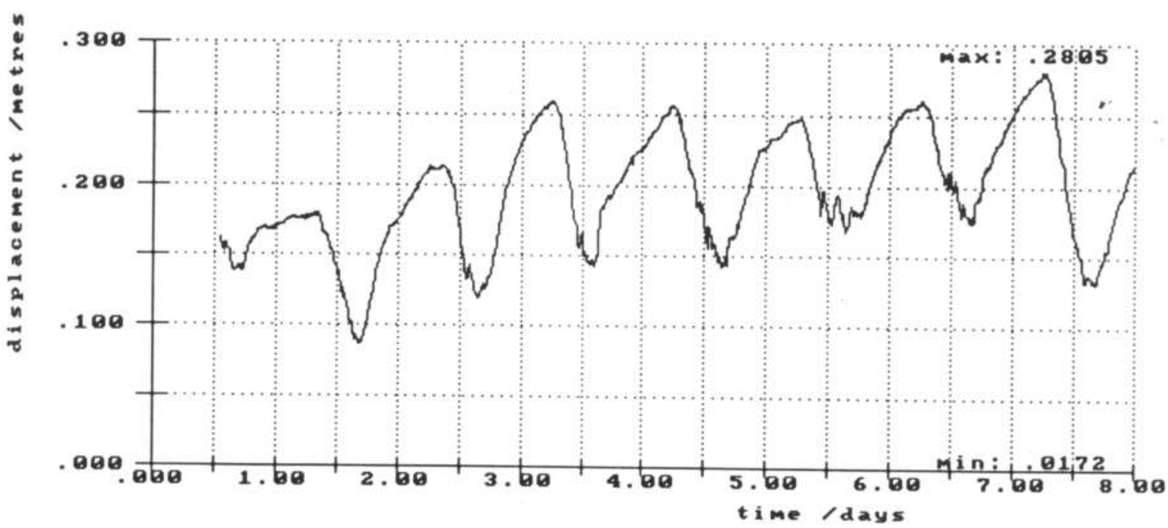

c) Longitudinal displacement away from Hessle tower

Fig. 11 The effect of temperature on deck displacement:

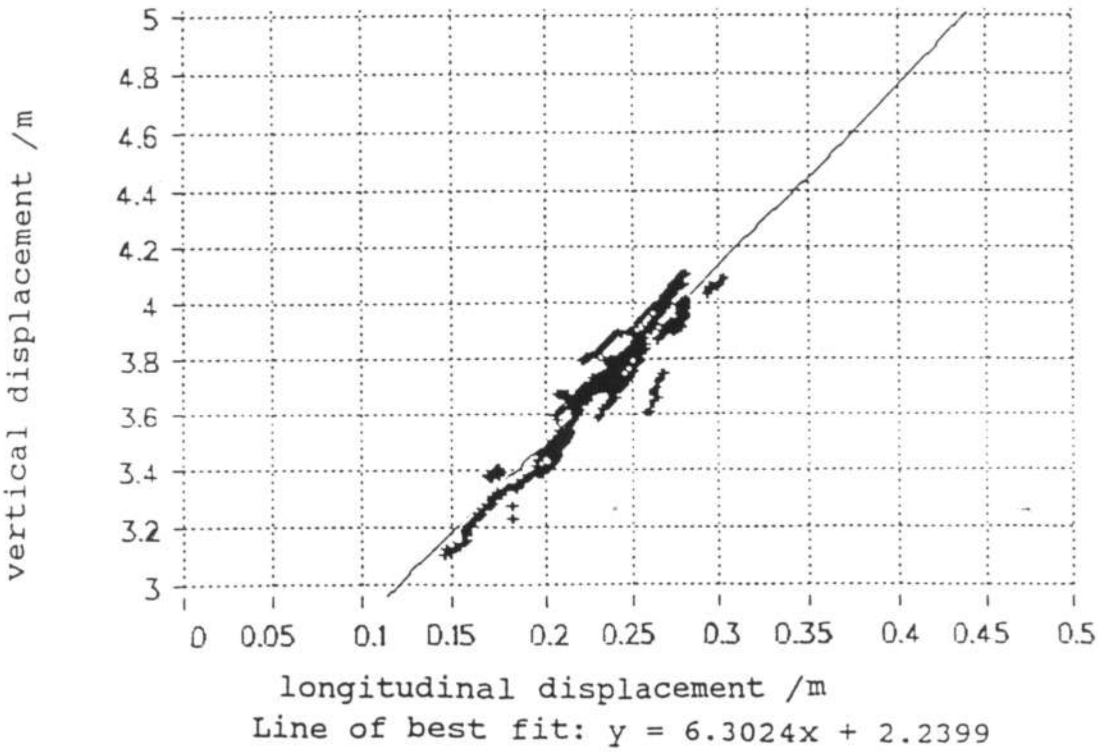

Fig. 12 Longitudinal displacement (away from tower) vs. vertical displacement

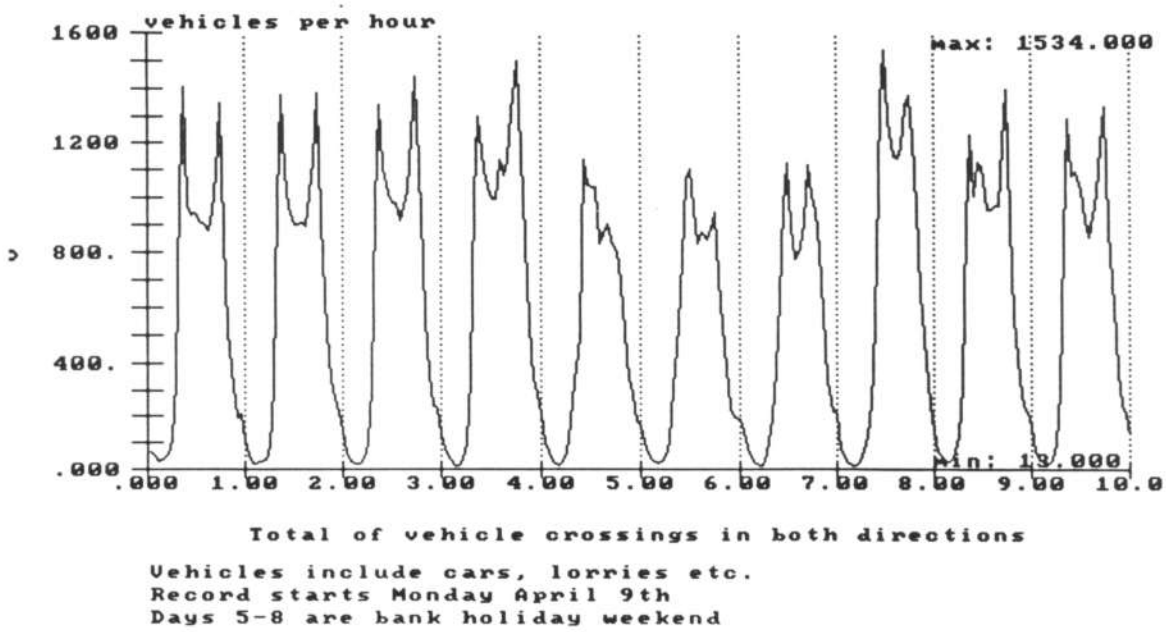

a) Total number of vehicles per hour

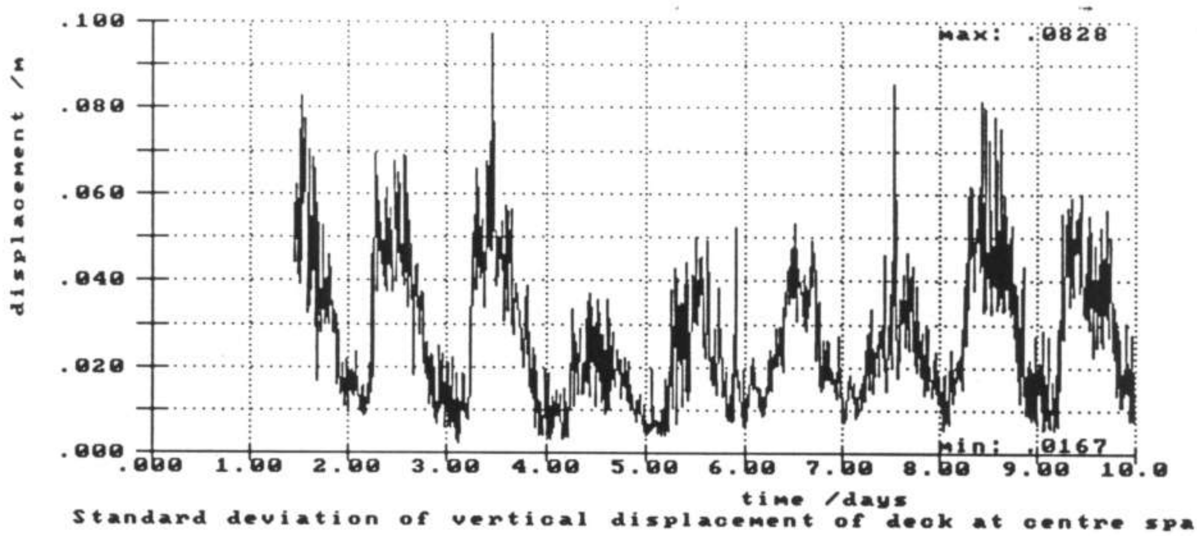

b) Standard deviations of vertical displacement

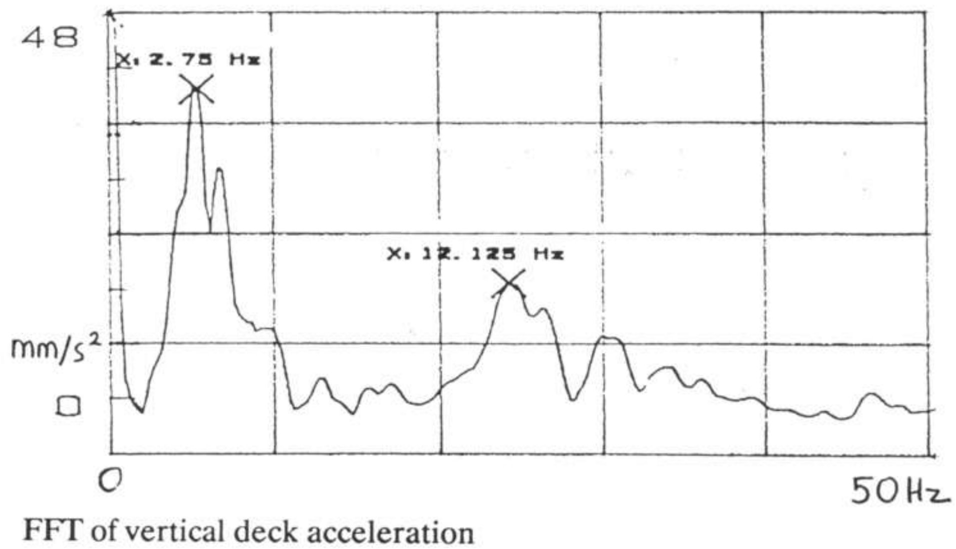

c) FFT of vertical deck acceleration

Fig. 15 Effect of traffic on quasi-static and dynamic response of Bridge during a 10-day period (including 3-day weekend)

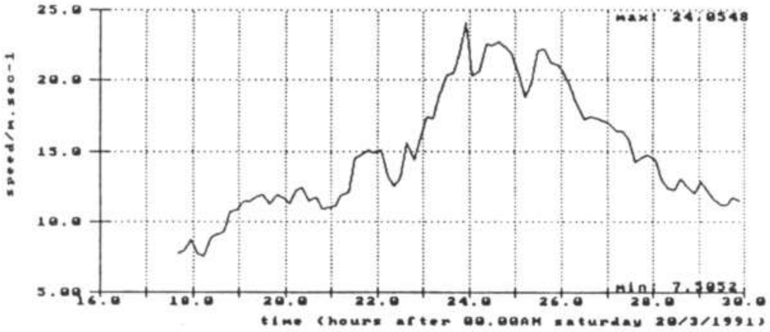

a) Wind speed V

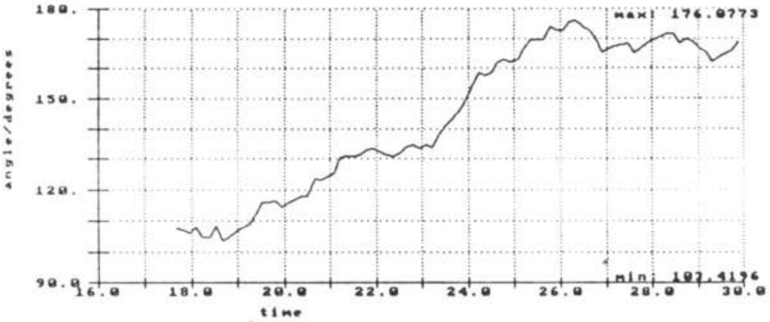

b) Wind bearing θ (West $\approx$ 180°)

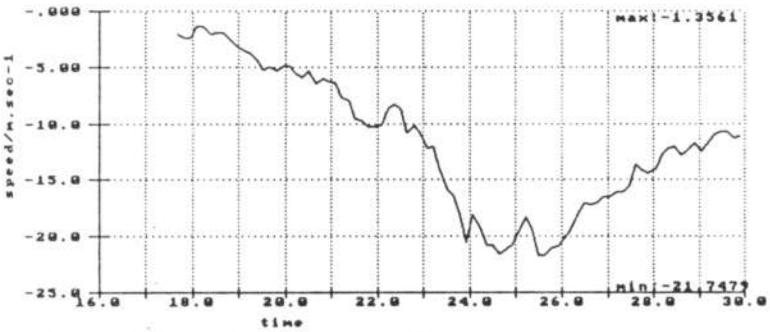

c) Normal component $V\cos\theta$

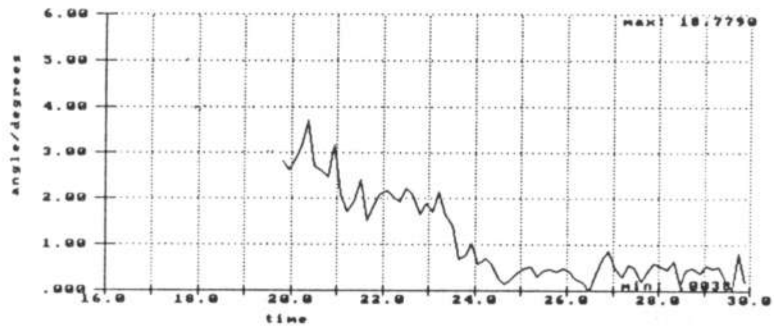

d) Vertical angle α (wind from above is +ve)

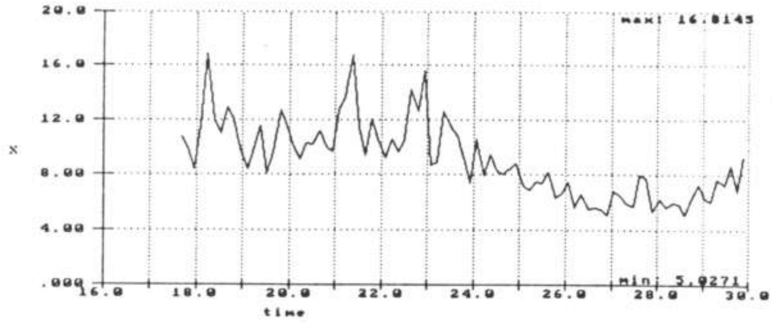

e) Turbulent intensity $\mathbf{I} = \sigma(V) / \mu(V)$

Fig. 16 Characteristic of wind during windy weekend

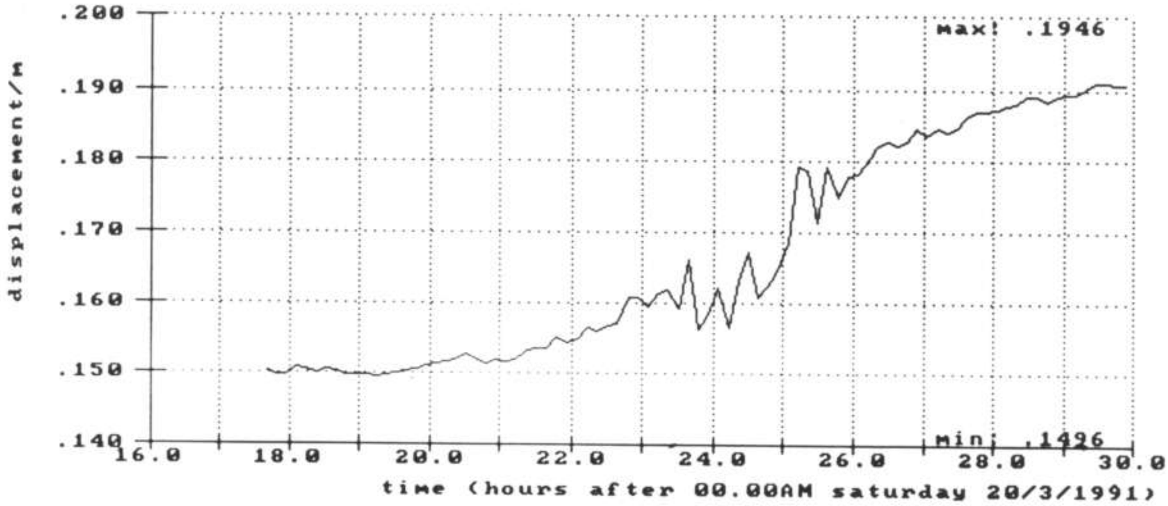

a) movement away from Hessle tower

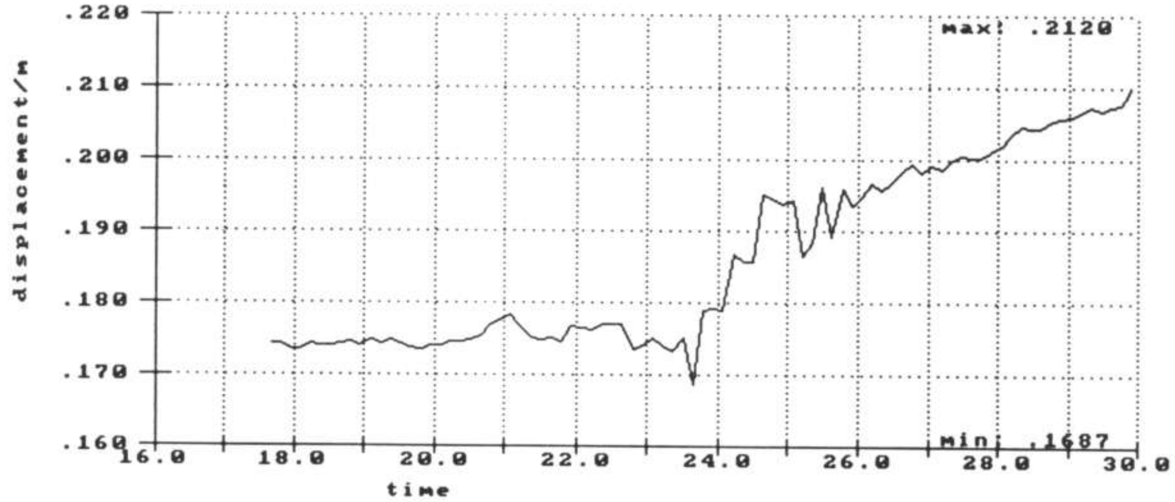

b) movement away from Barton tower

Fig. 17 Longitudinal displacement during windy weekend

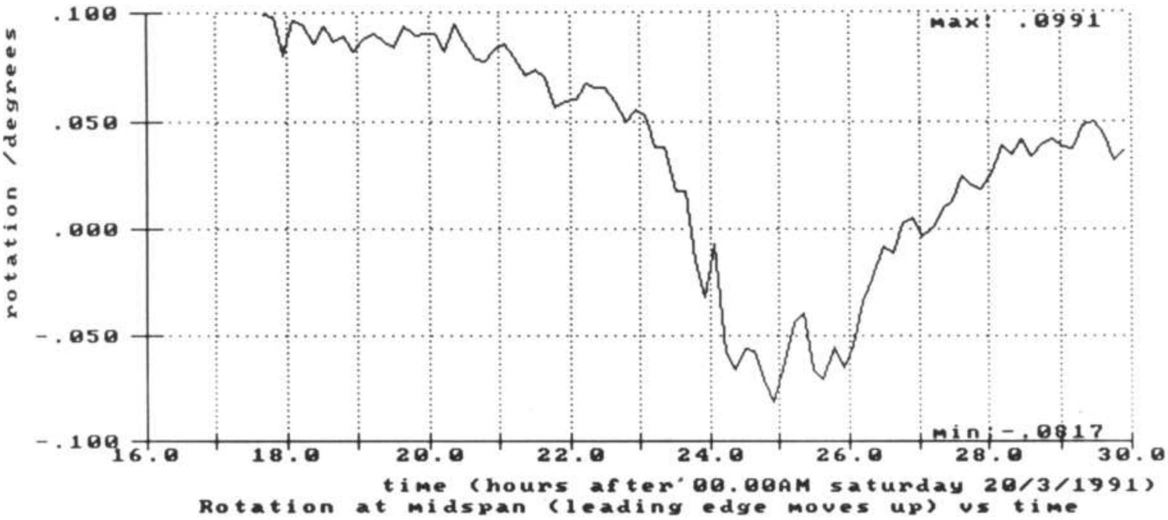

a) rotation as a function of time

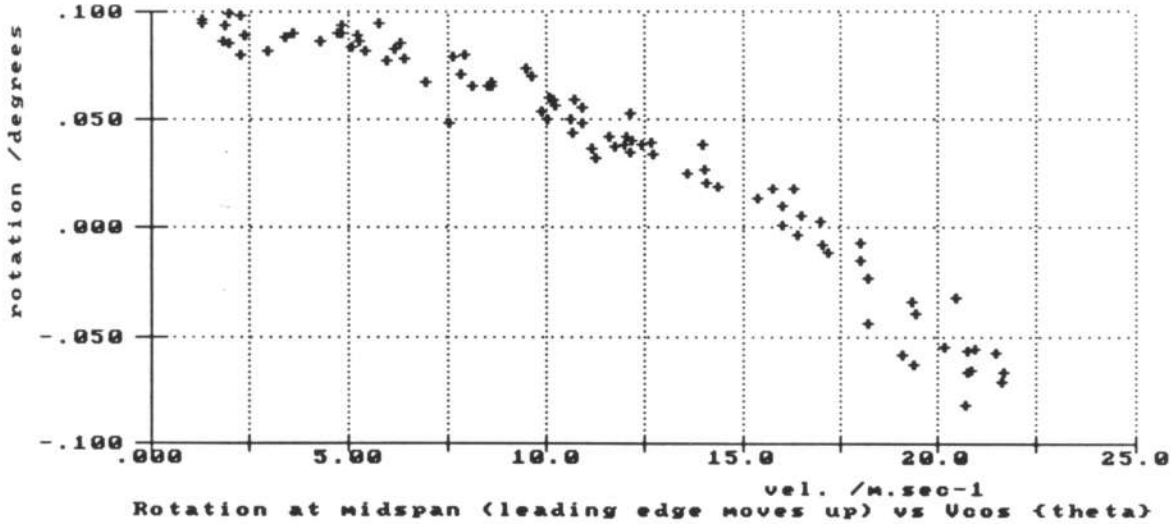

b) rotation as a function of wind speed

Fig. 18 Variation of deck rotation during windy weekend

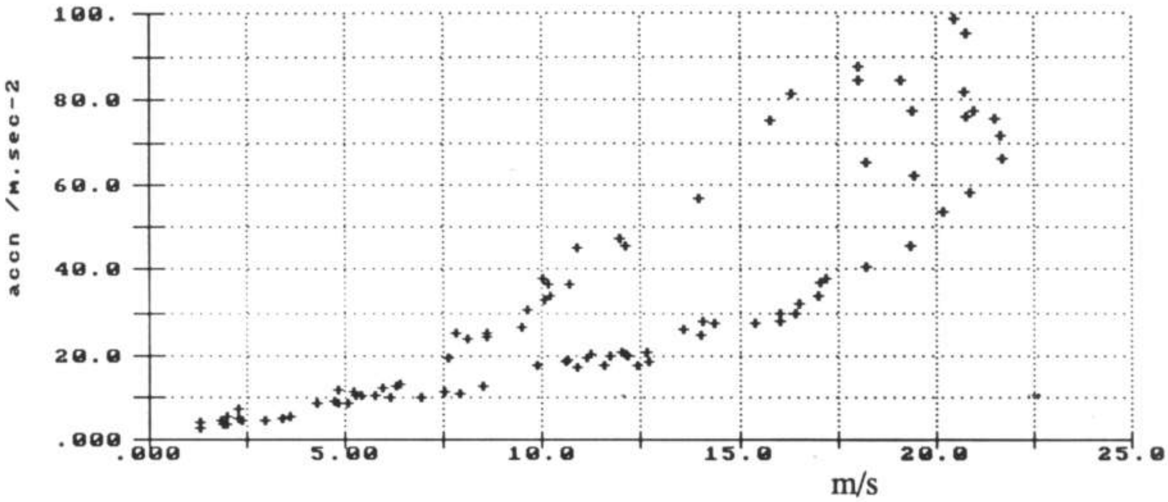

a) $\sigma(\ddot{y})$ vs $V\cos\theta$

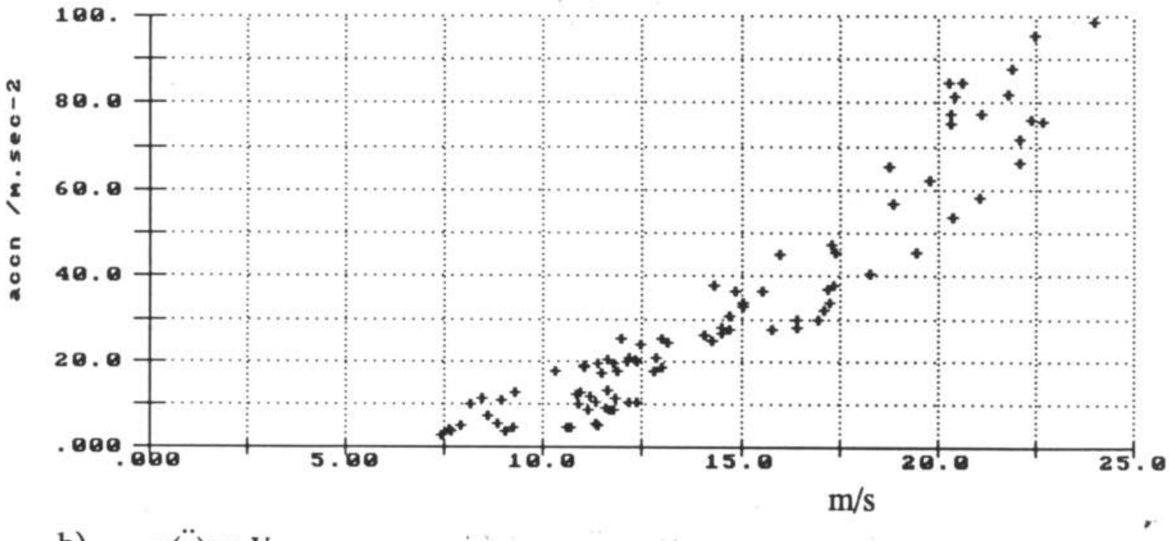

b) $\sigma(\ddot{y})$ vs V

Fig. 19 Standard deviation of vertical response in mode 1 (0.12Hz) during windy weekend

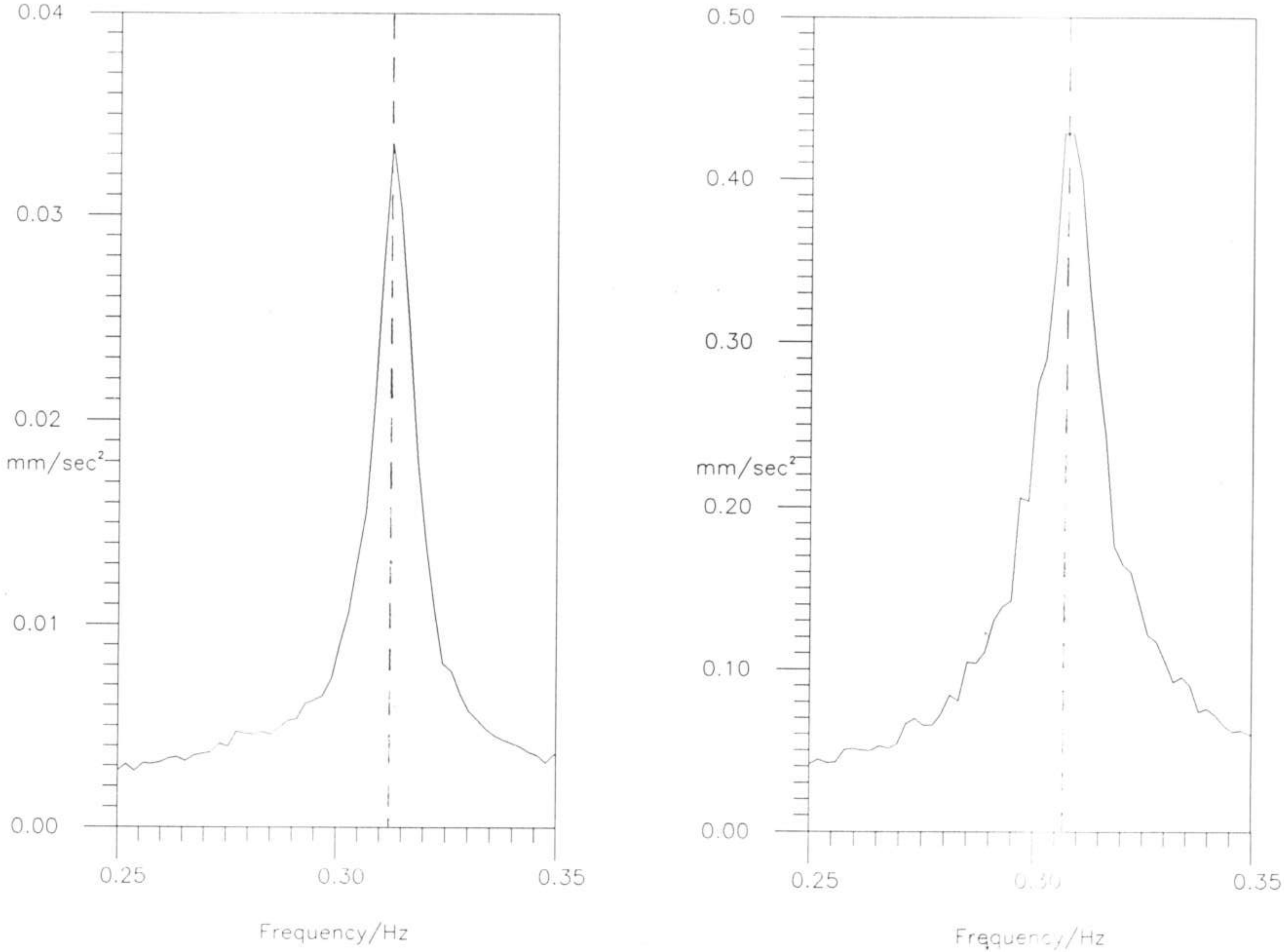

a) 0-2m/s wind speed band

b) 15-16.5m/s wind speed band

Fig. 20 Acceleration autopower spectrum for torsional mode T1 (0.31Hz) for different winds showing shifted frequency, damping and amplitude.